



## ORIGINAL ARTICLE

# Exploring the mechanism of *Artemisia argyi* chemical composition for ulcerative colitis based on network pharmacology



Menghe Li <sup>a,b,1</sup>, Jianghao Liu <sup>a,b,1</sup>, Caiwenjie La <sup>a,b</sup>, Tao Liu <sup>a,b</sup>, Zibo Zhao <sup>a,b</sup>, Zui Wang <sup>f</sup>, Minghui Dai <sup>a,b</sup>, Jiming Chen <sup>f</sup>, Zhe Ren <sup>a,b</sup>, Cuifang Ye <sup>a,b,\*</sup>, Yifei Wang <sup>a,b,c,d,e,\*</sup>

<sup>a</sup> Department of Cell Biology, College of Life Science and Technology, Jinan University, Guangzhou, China

<sup>b</sup> Guangdong Provincial Biotechnology Drug & Engineering Technology Research Center, Guangzhou, China

<sup>c</sup> GuangZhou (Jinan) Biomedical Research and Development Center Co. Ltd, Guangzhou, China

<sup>d</sup> Key Laboratory of Innovative Technology Research on Natural Products and Cosmetics Raw Materials, Guangzhou, China

<sup>e</sup> National Engineering Research Center for Modernization of Traditional Chinese Medicine- Artemisia Argyi Branch Center, Guangzhou, China

<sup>f</sup> Guangdong Provincial Engineering Center of Topical Precise Drug Delivery System, School of Pharmacy, Guangdong Pharmaceutical University, Guangzhou, China

Received 15 April 2023; accepted 31 May 2023

Available online 07 June 2023

## KEYWORDS

*Artemisia argyi*;  
Natural products;  
3β-ethoxytanaparholide;  
Network pharmacology

**Abstract** A persistent digestive disorder known as ulcerative colitis (UC) is characterized by a high rate of recurrence and a difficult road to full recovery. An herbal treatment with a long history of use in conventional Chinese medicine, *Artemisia argyi*, has shown encouraging results in preventing the return of clinical UC. We carried out an experiment to isolate and identify the small molecules in *Artemisia argyi* to investigate the chemical makeup of the therapeutic UC in this plant. Following an activity screen, we discovered that 3β-ethoxytanaparholide (ETP) had significantly greater anti-inflammatory action than the medicine we had chosen as a positive control, dexamethasone, and this is the first report of ETP in terms of biological activity. Systematic network pharmacological analysis confirmed that ETP acted on multiple targets during the pathogenesis of UC. These targets regulate a variety of UC-related signaling pathways, including but not limited to TNF, IL-17, and Ca<sup>2+</sup> signaling. Molecular dynamics simulations and MM-PBSA results showed that ETP was able

\* Corresponding authors at: Department of Cell Biology, College of Life Science and Technology, Jinan University, Guangzhou, China.

E-mail addresses: [cuifang\\_ye@163.com](mailto:cuifang_ye@163.com) (C. Ye), [twang-yf@163.com](mailto:twang-yf@163.com) (Y. Wang).

<sup>1</sup> These authors have contributed equally to this work and share the first authorship.

Peer review under responsibility of King Saud University



to form stable complexes with five targets, MMP1, MMP9, MUC1, S1PR1 and MMP12. The current work has previously shown the unknown anti-inflammatory ability of ETP and discovered that ETP can modulate various pathways throughout the development of UC to produce therapeutic advantages. These ground-breaking results highlight the urgent need for more analysis and development of ETP as a potential treatment plan for UC.

© 2023 The Author(s). Published by Elsevier B.V. on behalf of King Saud University. This is an open access article under the CC BY-NC-ND license (<http://creativecommons.org/licenses/by-nc-nd/4.0/>).

## 1. Introduction

UC, is a chronic idiopathic inflammatory bowel disease (IBD) in which patients need to take medications frequently to have normal lives (Ng et al., 2013). Corticosteroids, immunosuppressants, and TNF-alpha inhibitors are some of the modern drugs frequently prescribed to treat this condition (Toruner et al., 2008); (Lichtenstein et al., 2012). For UC patients, the severe side effects of these medications are magnified during the lengthy course of treatment.

Since ancient times, traditional Chinese medicine (TCM) has been used in China to treat inflammation, and research over time has proven that it has positive therapeutic results with few negative side effects (Fan et al., 2020). TCM may therefore give people with UC hope for potential treatment. Recent studies have confirmed the role of *Artemisia* plants in treating IBD. Research indicates that *Artemisia absinthium* were more effective than a placebo in inducing disease remission and preventing clinical recurrence following IBD surgery (Ng et al., 2013). Clinical randomized controlled trials have demonstrated that *Artemisia absinthium* therapy significantly reduced both disease activity and depressive symptoms in patients (Langhorst et al., 2015). It appears that *Artemisia* plants have tremendous potential in treating IBD. A significant herbal remedy with a >2000-year history of usage in China is *Artemisia argyi*. In the treatment philosophy of traditional Chinese medicine, *Artemisia argyi* leaves can be made into moxibustion and used to treat various diseases, including colitis, arthritis, asthma, dysmenorrhea, etc. Modern research indicates that the essential oil of *Artemisia argyi* contains abundant chemical components, including terpenoids, ketones, alcohols, acids, and alkyl hydrocarbons, and this essential oil has the potential to dose-dependently suppress the release of pro-inflammatory mediators such as prostaglandin, nitric oxide, reactive oxygen species, TNF- $\alpha$ , IL-6, IFN- $\beta$ , and monocyte chemokine. (Liu et al., 2021). This indicates that this herb plays an important role in the treatment of inflammation, but the primary ingredients and mechanisms of this herbal remedy for the treatment of ulcerative colitis are still unknown. Our earlier research revealed that this substance's essential oil has great anti-inflammatory properties and the ability to cure disorders connected to inflammation by preventing the activation of the NLRP3 inflammasome. (Chen et al., 2021). Further investigation revealed that this essential oil has high levels of beta-caryophyllene, which reduces macrophage ferroptosis and inflammation in experimental colitis. (Wu et al., 2022). Our research has confirmed the anti-inflammatory effect of *Artemisia argyi* and the therapeutic effect of its chemical component beta-caryophyllene on experimental colitis. However, compared to the abundant chemical components in *Artemisia*

*argyi*, our research is still far from sufficient. Further exploration of the chemical components of *Artemisia argyi* and their anti-inflammatory effects is needed, particularly in evaluating their potential for treating ulcerative colitis.

From the leaves of *Artemisia argyi*, we isolated 25 natural compounds, including monoterpenes, sesquiterpenes, flavonoids, phenols, and lipids. The anti-inflammatory activity screening revealed that Compound 2, a guaiacolactone (3 $\beta$ -ethoxytanaphtholide, ETP), had the largest anti-inflammatory impact, outperforming the positive control medication we used, dexamethasone. However, there are few published reports on ETP and no studies on its anti-inflammatory properties or molecular processes.

Network pharmacology, which has a very broad variety of applications, has become a significant tool for researching the pharmacological effects of traditional Chinese medicine. Network pharmacology is a crucial tool for early analyses of the biological activity of tiny molecules of natural origin. A clear indication of the binding between molecules and targets can be obtained, in particular, by molecular docking and molecular dynamics. Therefore, to examine the mechanism of action and targets of ETP for UC, we integrated a network pharmacology method with bioinformatics, genetic difference analysis, molecular docking, molecular dynamics simulation, and MM-PBSA. The flowchart is given in Fig. 1.

## 2. Materials and methods

### 2.1. General experimental procedures

On a Bruker AVANCE-600 in CDCl<sub>3</sub>, <sup>1</sup>H NMR (600 MHz) and <sup>13</sup>C NMR (150 MHz) results were obtained. Column chromatography was carried out using the following gels: silica gel (Qingdao Marine Chemical Ltd. Qingdao, P. R. China), Sephadex LH-20 gel (GE Healthcare, Sweden), YMC ODS-A-HG gel (50  $\mu$ m, YMC, Japan), and MCI gel (SaiPuRuiSi. Beijing, P. R. China). On an Agilent 1260 system, preparative HPLC separations were performed using a YMC-Pack ODS-A column (250  $\times$  10 mm, 5  $\mu$ m).

### 2.2. Plant material

In Nanyang, Henan Province, People's Republic of China, fresh leaves of *Artemisia argyi* (Asteraceae) were picked in May 2019 and air-dried. Professor Yifei Wang (College of Life Science and Technology, Jinan University) identified the plant specimen (No. 201905). At the Guangzhou Jinan Biomedicine Research and Development Center, Jinan University, a voucher specimen was placed.

### 2.3. Extraction and isolation

After soaking 200 kg of *Artemisia argyi* leaves in 10 times the volume of 95% ethanol 3 times and concentrating, 14.3 kg of crude ethanol extract was obtained. The crude ethanol extract was extracted with 3 times the volume of petroleum ether and ethyl acetate, resulting in 2.42 kg and 2.41 kg, respectively, of partial petroleum ether and partial ethyl acetate extracts. These extracts were purified into 25 different compounds after being repeatedly eluted by column chromatography using silica gel, AB-8 resin, MCI, ODS, and LH-20 gel columns. The specific separation processes for each of these 25 compounds are detailed in the [Supplementary Information](#).

### 2.4. Cell culture and treatment

RAW 264.7 cells were acquired from the Chinese Academy of Sciences Cell Bank in Shanghai, China. Cells were grown in DMEM (Dulbecco's Modified Eagle's Medium) with 10% Fetal Bovine Serum (FBS; Gibco, Grand Island, NY, USA; #10100-147) and 1% Penicillin-Streptomycin (#15070063; Gibco) in a humid environment at 37 °C with 5% CO<sub>2</sub>.

### 2.5. Cytotoxic activity

After being grown overnight in DMEM with 10% FBS at  $1.5 \times 10^5$  cells per well, RAW264.7 cells were subjected to a variety of ETP doses for 24 h. Then, 20  $\mu$ L MTT was added to each well, and the plate was incubated for 4 h at 37 °C in the dark. Then, the supernatant was removed, and each well was filled with 100  $\mu$ L of DMSO. Before recording the optical density (OD) at 490 nm with an enzyme immunoassay reader (Bio-Rad Laboratories, Inc., Hercules, CA, USA), the plates were gently shaken for 15 min at room temperature. The viability of the cells at each ETP concentration was compared to the viability of the control cells without ETP. The half-maximal toxic concentration (CC<sub>50</sub>) of each sample was determined from the graph of the inhibitory rate on the cell survival rate against the sample concentration. Assays were performed in triplicate, and the CC<sub>50</sub> values were calculated by GraphPad Prism 8.

### 2.6. Inhibition of NO production

With the use of the Griess reagent kit (Beyotime, Shanghai, China), NO production was indirectly measured. In 96-well plates,  $1.5 \times 10^5$  RAW 264.7 cells were plated per well, and the cells were grown for 24 h. The cells were then exposed to LPS (100 ng/mL) alone or in combination with the test sample for 18 h. Equal quantities of Griess reagents A and B were combined with the culture supernatants after being collected. After incubating for 10 min at room temperature, the absorbance was measured at 540 nm with a spectrophotometer (Bio-Rad Laboratories, Inc., Hercules, CA, USA). According to a standard calibration curve made from sodium nitrite, the quantity of NO was estimated. The 50% inhibition concentration (IC<sub>50</sub>) of each sample was determined from the graph of the inhibitory rate on NO production against sample concentration. Assays were performed in triplicate and the IC<sub>50</sub> values were calculated by GraphPad Prism 8.

### 2.7. Identification of ETP UC associated genes

It is necessary to gather all potential ETP action targets, integrate validated targets for ulcerative colitis, and take the overlapping portion of the two for further study to investigate the mechanism of ETP targeted therapy for ulcerative colitis. The Swiss Target Prediction database (<https://www.swisstargetprediction.ch>) (Gfeller et al., 2013), the PharmMapper webserver (<https://www.lilab-ecust.cn/pharmmapper/>) (Wang et al., 2017) and the TargetNet database (<https://targetnet.scb-dd.com>) (Yao et al., 2016) were employed to predict the potential targets of ETP.

In summary, the compounds were converted to Mol2 format and uploaded to the PharmMapper database, and Drugable Pharmacophore Models were selected as the Targets Set for prediction. Convert the compounds to SMILES format for Swiss Target Prediction and TargetNet databases. Homo sapiens was used for prediction in the Swiss Target Prediction tool, and Ensemble TargetNet was used for prediction in the TargetNet database. The GeneCards database (<https://www.genecards.org/>) (Stelzer et al., 2016), the DisGeNET database (<https://www.disgenet.org/>) (Piñero et al., 2021) and the OMIM database (<https://www.omim.org/>) (Amberger et al., 2015) were used to find a target for ulcerative colitis. In addition, we used ulcerative colitis as the keyword to search for related targets in three databases and set the relevance score > 10 in the GeneCards database and evidence index (EI) as 1 in the DisGeNET database.

### 2.8. GEO gene difference analysis

We used the GEO2R program to analyze the GSE179285 dataset of the GEO database (<https://www.ncbi.nlm.nih.gov/geo/>) to further screen the active components and their targets that were first screened (Barrett et al., 2013); (Keir et al., 2021) and further screen the targets by analyzing the genetic differences of GSE clinical samples. We selected the groups marked as Ulcerative Colitis in Diagnosis and inflamed in Inflammation as the UC disease group. Healthy control was set as the control group, and the significance level cutoff was set to 0.05.

### 2.9. Protein-protein interaction network (PPI)

The STRING database (<https://string-db.org/>) was used to create a protein-protein interaction network of important targets (Szklarczyk et al., 2021). The target organism chosen was Homo sapiens, and the evaluation standards were set at high confidence (>0.700). The exported PPI network was optimized in Cytoscape 3.8.0 (<https://cytoscape.org/>) (Shannon et al., 2003) to find more targets for ulcerative colitis screening.

### 2.10. GO and KEGG pathway enrichment analysis

The enrichment of biological processes (BP), cellular components (CC), and molecular functions (MF) in gene ontology (GO) analysis and Kyoto Encyclopedia of Genes and Genomes (KEGG) enrichment analysis were examined using the Metascape website (<https://metascape.org>) (Zhou et al., 2019). In summary, after submitting a gene list and selecting H. sapiens as the target species, the Pathway & Process Enrich-

ment analysis was customized with a P Value Cutoff of 0.01 and a Min Overlap and Min Enrichment set at 2.

### 2.11. Molecular docking

The molecular docking technique can be used to forecast the conditions and forces that will bind target small molecules to proteins. The RCSB database (<https://www.rcsb.org/>) (Protein Data Bank, 2019) (RCSB, 2019) contains the target protein. AutoDock Vina was used for further molecular docking (Trott and Olson, 2010); (Eberhardt et al., 2021). In conclusion, the protein that was retrieved from the RCSB database in Autodock was examined, the water molecules were removed, and the receptor hydrogen was given. The charge was determined and the atoms type was set to AD4. The ligand's Detect Root and Choose Torsions commands were executed. The Vina program was then used to perform docking. For visual analysis, further tools include Discovery Studio Visualizer 2021 (<https://discover.3ds.com/>) and PyMOL (<https://pymol.org/edu/>) (Seeliger and de Groot, 2010).

### 2.12. Molecular dynamics simulation

We further confirmed the results using a molecular dynamics simulation based on the outcomes of molecular docking and gene expression differential analysis. Briefly, the tleap tool in AmberTools22 was first used to create the input files for the ligands (Case et al., 2022). The ligands were then transformed into input files for the gromacs using the acpype program, with the receptors being represented by the AMBER14SB force field and the ligands by the gaff force field (Sousa da Silva et al., 2012). The MD process was completed by Gromacs software (Abraham et al., 2015). The entire simulation was run using the TIP3P water model, and during the equilibrium simulation state, which lasted 100 ps and involved an MD simulation lasting 100 ns, the temperature and pressure were both kept constant at 310 K and 1 bar, respectively. Using the Gromacs tool, the simulation results were examined and shown.

### 2.13. Molecular mechanic/Poisson-Boltzmann surface area (MM-PBSA) calculation

Utilizing trajectory data from molecular dynamics simulations, the relative binding energy of protein–ligand complexes was computed using the gmx\_mmpbsa tool (Valdés-Tresanco et al., 2021). We used the trajectories recorded between 80 and 100 ns for computation of the combined free energy based on the stability of the simulated process. The binding affinity was characterized by analyzing the binding energy, van der Waals energy, electrostatic energy, polar solvation energy, and SASA energy data. The decomposition of energy into residues was conducted to identify the key residues involved in the binding process.

## 3. Results

### 3.1. Structural identification of compounds

The compounds we isolated were all known compounds, as indicated by analysis of the NMR data, and their structures

were validated by comparison with some recorded literature as (1*R*,5*R*,7*R*)-1,5-dihydroxygermacra-4(15),10(14),11(12)-triene (Zhao et al., 2014), 3β-ethoxytanaparthalide (Ke et al., 2012); 3 β-hydroxy-13-acetoxygermacra-1(10)*E*,4*E*, 7(11)-triene-12,6α-olide (Zdero and Bohlmann, 1990); 1 α,3α,4β-tri hydroxy-8α-acetoxyguai-9,11(13)- dien-6α,12-olide (Ahmed et al., 2004); (*S*)-8-hydroxycarvotanacetone (Sousa et al., 2020), 4-hydroxypiperitenone (Jiang et al., 2022); (*S*)-2-(4-methyl-5-methylenecyclohex-3-en-1-yl)propan-2-ol (Yrjänheikki, 1980); perillaldehyde (Craveir and Vieira, 1992), di-isobutyl phthalate (Shi and Han 1996), 7-methoxy coumarin (Benkiki et al., 2007), 8-hydroxy-5,6,7-trimethoxycoumarin (Shuhua et al., 2004), 4,6-dihydroxy-2 -methoxyacetophenone (Brown, 1992), methyl p-hydroxycinnamate (Hiraga et al., 1996), 3,4-dimethoxyacetophenone (Li et al., 2015); matrixisobenzofuran (Iverson et al., 2010); 1-[(4*S*-3,4-dihydro-4-hydroxy-2,2-dimethyl-2H-1-benzopyran-6-yl)]-ethanone (Kang et al., 2016); euparin (Habtemariam, 2001); naringenin (Li et al., 2007), Hispidulin (Marques et al., 2010); apigenin (Silva et al., 2015); Spinacetin (Formisano et al., 2012); arctigenin (Higashinakasu et al., 2005), (+)-Pinoresinol (Xu et al., 2008), methyl 4,5- didehydrojasmonate (Kiyota et al., 1997); hydroxydihydrobovalide (Zhang et al., 2014). Detailed NMR data are described in the Supplementary Data (See Fig. 2).

### 3.2. Cytotoxicity and NO inhibition ability of compounds

Using the RAW264.7 cell line, we evaluated the cytotoxicity of various substances in this investigation. We also conducted tests for anti-inflammatory activity within acceptable dosage ranges. In the presence of LPS-induced cellular inflammation, our results show that ETP exhibits strong anti-inflammatory effects, with an IC<sub>50</sub> of 0.5 ± 0.1 μM (Table 1 and Fig. 3).

### 3.3. Identifying the targets of ETP action on UC

To find prospective targets for the treatment of ETP and UC, we used a range of computational tools and databases, including PharmMapper, Swisstarget, Targetnet, Genecards, Disgenet, and OMIM. We discovered 191 overlapping targets between ETP and UC by using the Venn diagram analysis technique. After performing a differential gene expression study, we identified a total of 25 targets that showed appreciable up- or downregulation at the beginning of UC. The goal of this selection was to discover possible therapeutic approaches for both ETP and UC. These 25 targets were then subjected to additional screening and analysis (Fig. 4).

### 3.4. Construction of protein–protein interaction (PPI) networks

The 25 targets identified throughout the screening phase were evaluated for protein–protein interaction (PPI) networks to identify important targets. ADA, CASP1, ME1, TBXAS1, and TGM2 were the only five targets that did not interact in the resulting network. Additionally, as shown in Fig. 5, none of the five downregulated targets (ABCG2, ABCB1, NR1H4, CYP3A4, and CYP2C9) showed any relationship with the complete network. As a result, we decided not to analyze these targets further and used the remaining 15 targets to create a different interaction network for later evaluations.

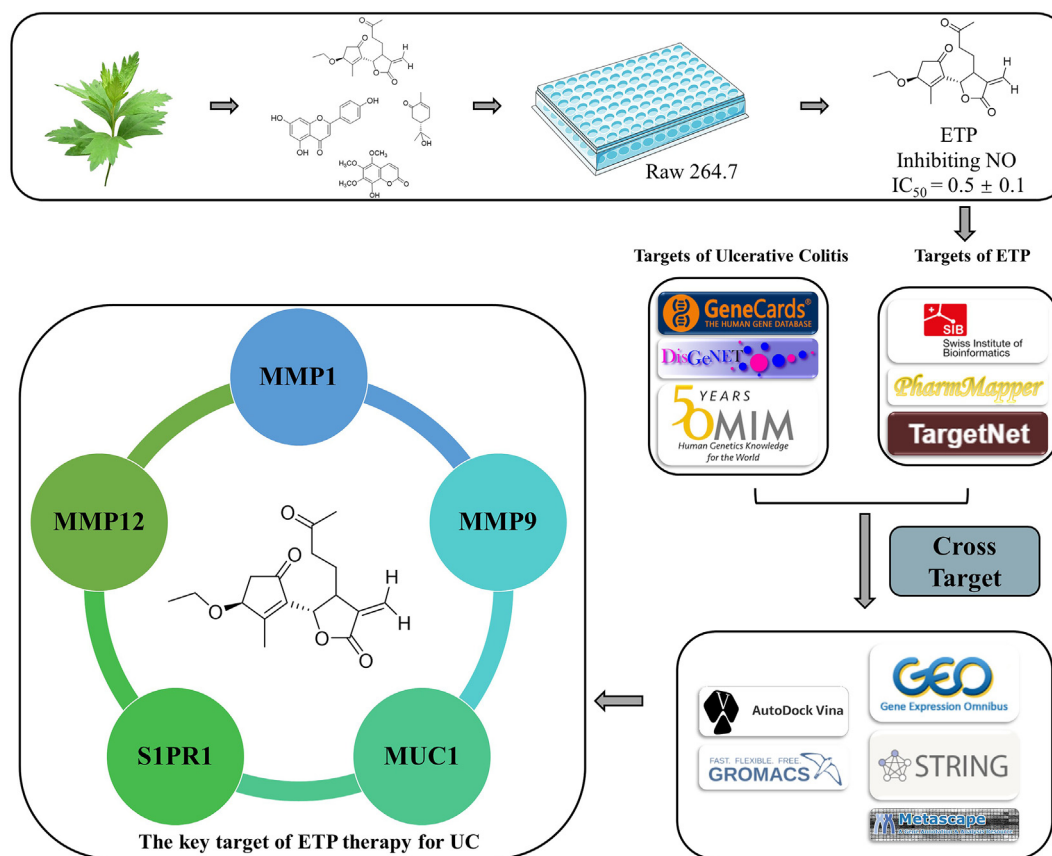


Fig. 1 Workflow of this study.

### 3.5. GO and KEGG enrichment analysis

The present study examined 15 identified genes using Gene Ontology (GO) annotation and discovered that ETP significantly affects a number of biological processes, including cellular response to cytokine stimulation, collagen catabolic processes, positive regulation of cell migration, and response to hypoxia. ETP also has an impact on the extracellular matrix and external encapsulating, two cellular components. The modulation of many activities, including peptidase, endopeptidase, serine hydrolase, serine-type endopeptidase, serine-type peptidase, metallopeptidase, and metalloendopeptidase, is reflected in the molecular function of ETP. KEGG analysis showed that ETP significantly affects a number of pathways, including the TNF signaling pathway, the IL-17 signaling pathway, lipids and atherosclerosis, pathways in cancer, rheumatoid arthritis, leukocyte transendothelial migration, relaxin signaling pathway, fluid shear stress and atherosclerosis, transcriptional misregulation in cancer, human T-cell leukemia virus 1 infection, prostate cancer, and the calcium signaling pathway (Fig. 6).

### 3.6. Analysis of molecular docking results

In this study, molecular docking analysis was used to examine how ETP binds to the primary target. Indicating the prospect of ETP serving as a multitarget-acting active chemical, the acquired docking data showed binding energies that

were  $< 5.0$  kcal/mol for 14 targets, representing good binding between the receptor and the ligand (Wang et al., 2022). (Table 2 and Fig. 7). The best nine compound-target complexes with binding energies under  $-7.7$  kcal/mol were chosen after the molecular docking findings were ranked. Before being used in molecular dynamics simulations, these data were further examined using PyMOL and Discovery Studio Visualizer, visualized, and checked for accuracy (Fig. 8). (See Fig. 9)

### 3.7. Analysis of molecular dynamics simulation results

Molecular dynamics simulations are used to provide evidence on the stability of protein–ligand interactions. Using simulations lasting 100 ns and data collected from the docking results, the study focuses on the binding of ETP to nine different targets (MMP9, CD38, MMP12, MMP3, SIPR1, JAK3, MUC1, and MMP1). By assessing variables such as root mean square deviation (RMSD), hydrogen bonding, and binding free energy, one can assess the stability of ETP binding with the targets under discussion

#### 3.7.1. Root mean square deviation

The root mean square deviation (RMSD), which gauges how much an atom has deviated from its starting position, can be used to assess the stability of protein and ligand binding. Typically, lower deviations signify a more stable conformation. Here, we evaluate the stability of binding based on the standard of RMSD fluctuations within 1 Å (Eldehna et al.,

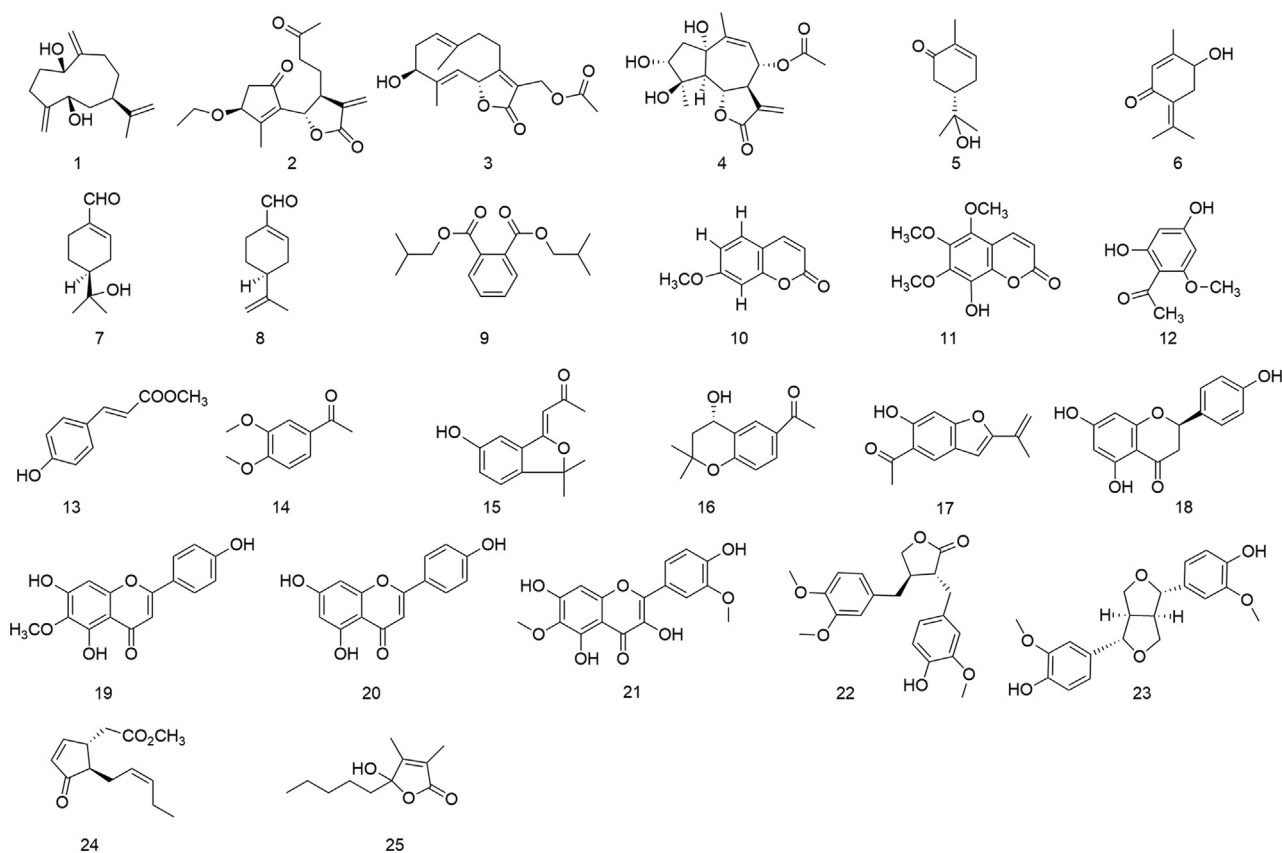


Fig. 2 Structures of Compounds 1–25.

**Table 1** Anti-inflammatory effects of active compounds on NO production in LPS-stimulated RAW 264.7 cells (n = 3).

Compound	IC <sub>50</sub> /μM <sup>a</sup>	CC <sub>50</sub> /μM <sup>b</sup>
2	0.5 ± 0.1	> 10
13	44.8 ± 0.1	> 100
14	93.3 ± 0.2	> 100
22	91.15 ± 0.3	> 100
Dexamethasone	4.1 ± 0.2	–

IC<sub>50</sub>, the half-maximal inhibitory concentration, values were expressed as the means ± SDs.

CC<sub>50</sub>, the half-maximal toxic concentration.

2021). Fig. 9 shows how we examined the variation in RMSD values for nine distinct complexes in this investigation. The findings revealed that ETP was able to maintain a comparatively stable conformation for the full 100 ns in the simulations with CD38 and MMP1 (Fig. 9B and I). However, MMP9, MMP12, MMP3, and MUC1 showed periodic changes (Fig. 9A, C, D, and G). After 50 ns, 70 ns, and 60 ns for S1PR1, JAK3, and CXCR4, respectively, a stable conformation was finally attained (Fig. 9E, F, H). It is interesting to note that imbalances between S1PR1 and CXCR4 during the initial simulation phase were associated with protein stability (Fig. 9E, H). During the simulation time, all seven remaining target proteins remained in their stable conformation.

### 3.7.2. Intermolecular hydrogen bonding analysis

Throughout the simulation, the hydrogen bonding analysis tool from Gromacs (shown in Fig. 10) was used to thoroughly examine the hydrogen bonding interactions between ETP and numerous target proteins. It is significant to note that since the binding between S1PR1 and ETP does not rely on hydrogen bonding, this figure is not given. As shown in Fig. 10A, F, G, and H, the results showed that ETP established persistent hydrogen bonds with MMP9, MUC1, CXCR4, and MMP1, particularly with MMP9, MUC1, and MMP1. Meanwhile, the hydrogen bond map (shown in Fig. 10B, E) revealed that CD38 and JAK3 were involved in the dissolution and reestablishment of hydrogen bonds during the process of reaching a new equilibrium. The fact that ETP and JAK3 failed to produce stable hydrogen bonds after achieving a new equilibrium state after 70 ns indicates that the final equilibrium state was not dependent on hydrogen bonds. Additionally, even though hydrogen bonds were created during the modeling of ETP using MMP12 and MMP3, the continuity of these interactions was not strong (as shown in Fig. 10C, D).

### 3.7.3. Analysis of MM-PBSA results

The MM-PBSA method can be used to calculate the binding energy between protein–ligand complexes, and the final calculation results can reflect the protein–ligand binding ability to some extent. From the calculation results (Table 3 and Fig. 11), the binding energy of ETP with MMP12 and

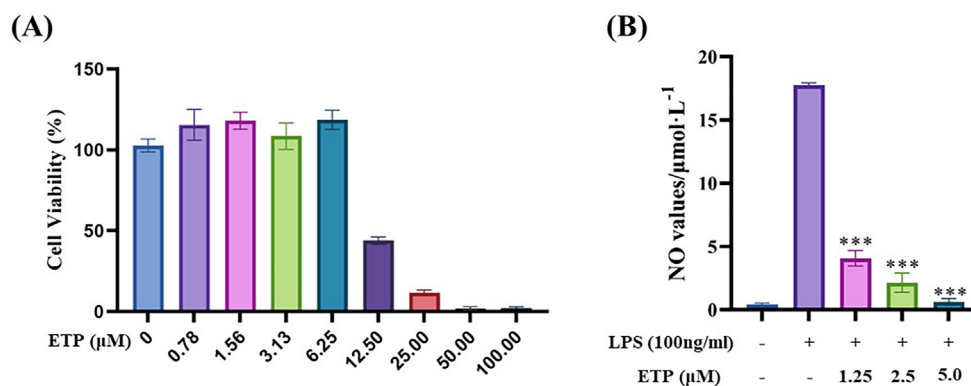


**Fig. 3** Cytotoxicity and NO inhibition ability of ETP. (A) Cytotoxicity of ETP on RAW264.7 cells (B) NO inhibition ability of ETP in LPS-stimulated cells. (\* $P < 0.05$ , \*\* $P < 0.01$ , \*\*\* $P < 0.001$  compared with LPS-induced group).

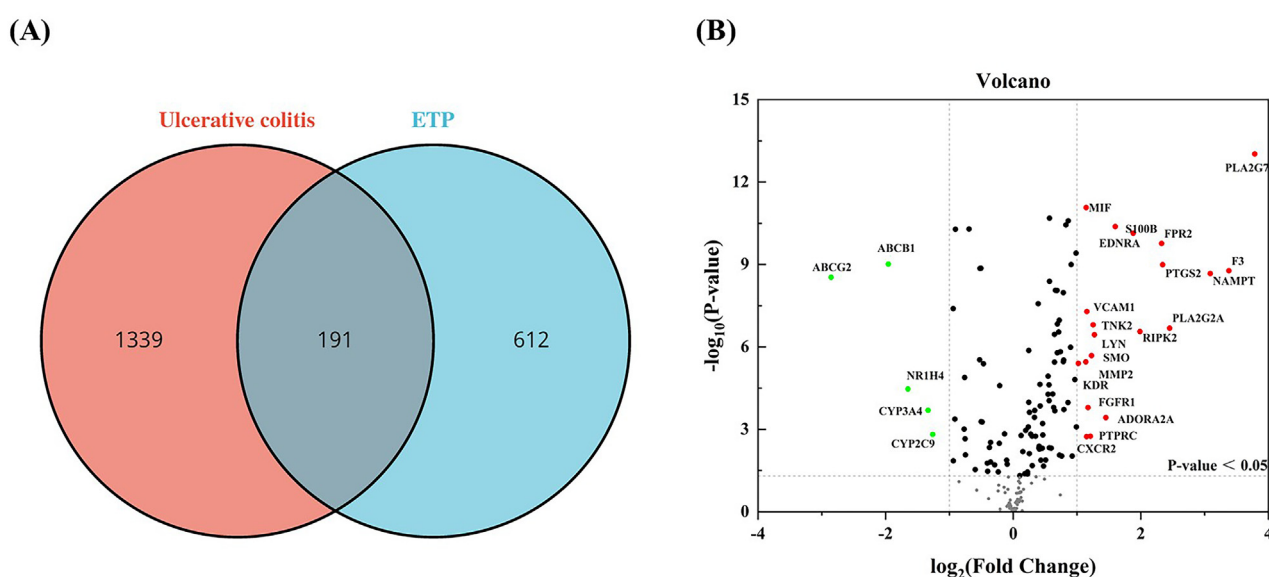


**Fig. 4** Intersection of UC targets and ETP targets. (A) Venn diagram depicting intersecting genes in UC/ETP (B) Volcano-plot representation of differential gene expression.

S1PR1 was the lowest ( $< -90$  kJ/mol), followed by MMP1 and MMP9 ( $< -80$  kJ/mol). The binding to MMP3, JAK3, and CXCR4 was relatively weak ( $> -60$  kJ/mol). The binding energy was further broken down to each residue for analysis (Fig. 12), and the results showed that TYR-240 plays a key role in the binding of ETP to MMP12 (Fig. 12C), and several residues play an active role in the binding to S1PR1 and MMP1, but GLU-121 in S1PR1 and ARG-214 in MMP1 are detrimental to their binding (Fig. 12E, I). Meanwhile, there are obvious key residues that play a role in the binding of ETP to MMP9, CD38, MMP3, and MUC1 (Fig. 12A, B, D, and G). However, several residues played a negative role in the binding of ETP to JAK3 and CXCR4, which was the key reason for the weak binding energy of ETP to these two target proteins (Fig. 12F, H).

#### 4. Discussion

ETP, is a guaiacolactone whose structure was first reported by Ke et al. (Ke et al., 2012). However, no relevant reports, either

chemical composition studies or biological activity studies, have been reported in this decade or so. Fortunately, ETP was again isolated from *Artemisia argyi* and showed a strong anti-inflammatory capacity in our study. Interestingly, when we examined the biological functions of ETP analogs, we discovered that they also have respectable anti-inflammatory properties. The Nrf2 activator *iso-seco-tanaparthalide* has been demonstrated to have anti-inflammatory properties both in vitro and in vivo in the LPS-induced sepsis model (Zhu et al., 2022). Meanwhile, 3-methoxytanaparthalide has been identified by researchers as an inhibitor of NF- $\kappa$ B (Jin et al., 2004). These findings emphasize the possibility for more research by partially demonstrating the anti-inflammatory properties of this diterpene skeleton. Based on the extraordinary anti-inflammatory activity of ETP, we used a network pharmacology approach to explore the possible molecular mechanisms of its treatment of UC.

We first obtained 191 cross-targets of ETP and UC, and identified 15 core targets for further analysis and discussion through differential gene expression analysis and PPI network.

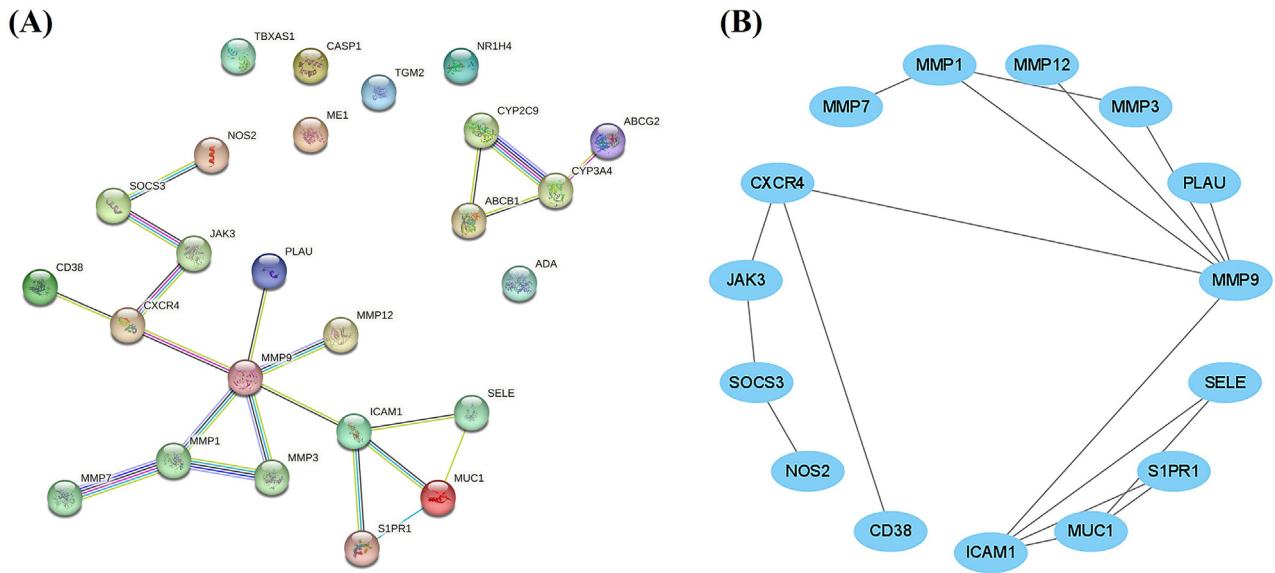


**Fig. 5** PPI network (A). PPI network with 29 targets (B). PPI network with 15 targets. In Figure B, nodes that are not related to the network from Figure A have been removed.

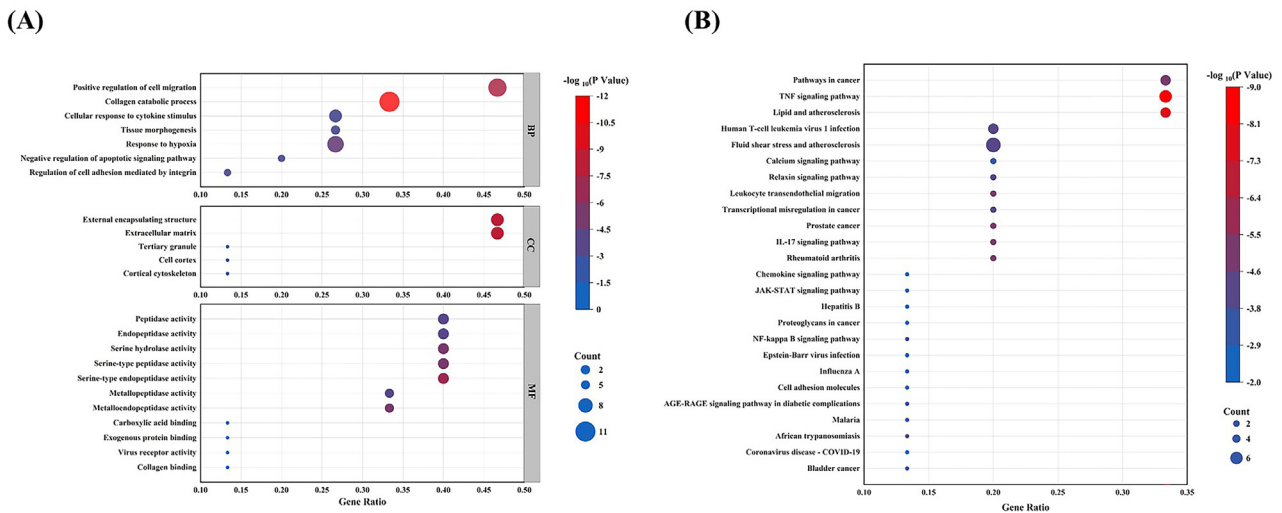


**Fig. 6** Results of GO enrichment analysis and KEGG enrichment analysis. (A) Gene ontology analysis of key intersecting genes of ETP and UC. (B) Kyoto Encyclopedia of Genes and Genomes (KEGG) pathway of key intersecting genes of ETP and UC. The color scale in the diagram represents  $-\log_{10}(P \text{ Value})$ , and the size of the dots represents the number of enriched genes.

The matrix metalloproteinases MMP1, MMP3, MMP7, MMP9, and MMP12 are all significantly upregulated when IBD first manifests, particularly MMP1 and MMP3, whose expression levels rise by almost 15 times (von Lampe et al., 2000). Excessive extracellular matrix hydrolysis and ulcer development in the presence of sick colonic mucosa have both been associated with MMP1 overexpression. Given these findings, various researchers have recommended MMP1 inhibitors as a potential treatment approach. The management of ulcerative diseases linked to MMP1 dysregulation may benefit from more research into the effectiveness and safety of MMP1 inhibitors (Wang and Yan, 2006). The cleavage of some medications is caused by MMP3 and MMP12, according to histological evaluations of patients. Importantly, after coincu-

bation with MMP inhibitors, such medicines recovered their inhibitory effect against TNF. These findings highlight the potential importance of MMP inhibitors in the treatment of disorders where MMP-mediated proteolysis plays a key role and offer insightful information on the mechanisms of action of specific medications (Biancheri et al., 2015). The overexpression of MMP7, which has been demonstrated to cleave Claudin-7, is closely related to inflammatory infiltration and mucosal erosion. The intestinal barrier becomes compromised as a result of this proteolytic activity, which in turn exacerbates the inflammatory response in IBD. Inhibiting MMP7 may be a novel therapeutic approach for the treatment of IBD given its role in disease development (Xiao et al., 2022). A substantial increase in MMP9 levels is connected to neutrophil infiltration.

**Table 2** Molecular docking results of ETP with key targets.

Target protein	PDB ID	Affinity (kcal/mol)
MMP9	4WZV	-8.3
CD38	2I65	-8.2
MMP12	1JK3	-8.1
MMP3	1B8Y	-7.9
S1PR1	3V2Y	-7.9
JAK3	3LXK	-7.8
MUC1	6TGG	-7.8
CXCR4	3OE8	-7.7
MMP1	1HFC	-7.7
MMP7	1MMQ	-7.2
NOS2	3E7G	-7.2
PLAU	1EJN	-6.3
ICAM1	5MZA	-5.8
SELE	1G1T	-5.8
SOCS3	2HMH	-4.5

In models of UC, experimental studies have shown that MMP9 ablation or suppression of its function by certain inhibitors can lessen disease severity and tissue damage. These findings highlight the role of MMP9 in the emergence of UC and open up interesting options for the creation of innovative therapies that target MMP9 for the treatment of UC patients (Castaneda et al., 2005); (Marshall et al., 2015). T-cell activation and proliferation are thought to be mediated by the catabolic enzyme CD38, which is involved in the metabolism of nicotinamide adenine dinucleotide. The inhibition of nicotinamide phosphoribosyl transferase (NAMPT), an upstream regulator of CD38, has been shown to be an efficient way to diminish CD38 activity, which in turn inhibits the immune response and reduces intestinal inflammation. These findings highlight the role of CD38 in the pathophysiology of inflammatory disorders and imply that altering the NAMPT-CD38 axis may be a feasible strategy for treating such conditions

(Gerner et al., 2018). Sphingosine-1-phosphate (S1P) has been demonstrated to promote the synthesis of IL-6 and maintain the activation of STAT3, which in turn causes S1PR1 to be upregulated. S1PR1 serves as a major receptor for S1P. Exploratory investigations have shown that inhibiting the NF-kappaB/IL-6/STAT3 signaling cascade and lowering S1PR1 expression can significantly improve symptoms in people with UC and colon cancer (Liang et al., 2013). The Janus kinase (JAK) family includes JAK3, a vital component that is largely expressed in hematopoietic cells and has been linked to the pathophysiology of a number of inflammatory diseases. Tofacitinib is a notable example of a JAK3 small-molecule inhibitor that has been licensed for the treatment of IBD, and has shown efficacy in lowering the inflammatory response linked to these disorders. These findings highlight the therapeutic utility of JAK3 inhibitors in treating these conditions (Roskoski, 2016); (Pérez-Jeldres et al., 2019). MUC1, a tumor-associated antigen that is ectopically produced in people with IBD, has been demonstrated to have significant impacts on connexins and cell polarity proteins, ultimately contributing to the disruption of intestinal barrier function. These results highlight the potential of MUC1 as a novel therapeutic target for the treatment of IBD by focusing on the underlying pathophysiology of the condition. Therefore, current studies aimed at better understanding the mechanisms behind the connection between MUC1 and IBD may open the door to the creation of novel therapeutic approaches (Breugelmanns et al., 2020). The CXCL12/CXCR4 interaction is thought to have a role in the pathogenesis of a wide variety of inflammatory diseases, and in patients with colitis, the expression levels of CXCR4 are directly correlated with the severity and scope of the disease. The promise of CXCR4 as a promising target for the development of novel medicines for treating patients with inflammatory disorders has been further supported by experimental results showing the effectiveness of CXCR4 antagonists in reducing symptoms of colitis in animal models (Mikami et al., 2008). As a crucial messenger

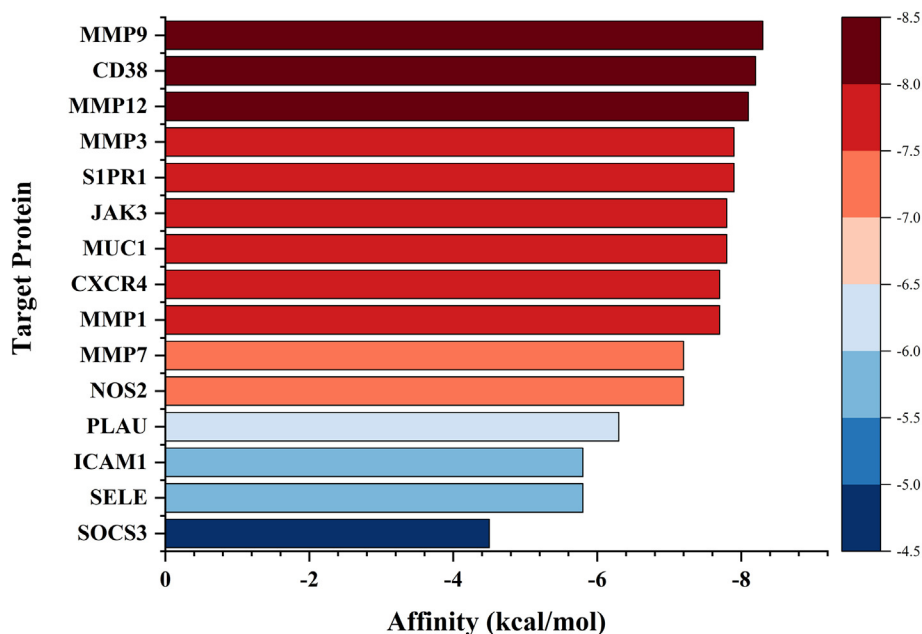


**Fig. 7** Molecular docking results of ETP with key targets. The color scale in the diagram represents the size of the affinity.

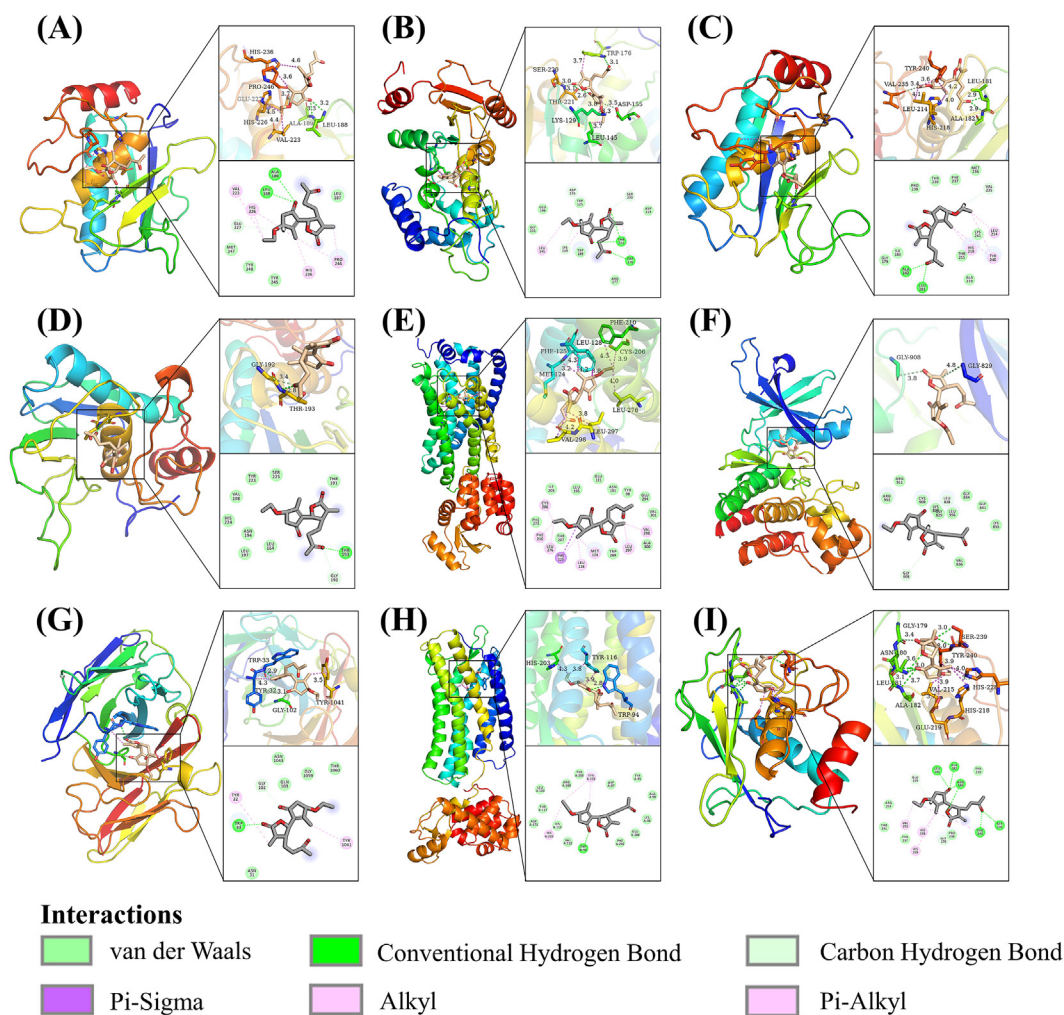


**Fig. 8** Molecular docking pattern of ETP and 9 targets. (A) ETP-MMP9. (B) ETP-CD38. (C) ETP-MMP12. (D) ETP-MMP3. (E) ETP-S1PR1. (F) ETP-JAK3. (G) ETP-MUC1. (H) ETP-CXCR4. (I) ETP-MMP1. All amino acids that interact with ETP are indicated in the picture, and the varying colors of the dashed lines denote various types of interactions.

molecule, nitric oxide (NO) is produced in greater quantities in individuals with IBD because of increased NOS2 expression and catalytic activity. There is strong evidence that UC disease activity and NOS2-derived NO levels are directly correlated. The therapeutic value of NOS2 inhibition in reducing symptoms of inflammatory bowel disease has been confirmed by experimental research (Kriegelstein et al., 2001). PLAU is involved in the inflammatory response and increases during aging as a biomarker of the aging process, but the ability of PLAU inhibition to alleviate UC symptoms has not been confirmed by studies (Wan et al., 2022). A growing body of research has shown that the vascular endothelium is essential for controlling leukocyte accumulation and distribution in inflamed tissues, with surface molecules such as ICAM1 and SELE serving as important examples of those involved in leukocyte adhesion and migration. Therefore, ICAM1 and SELE targeting may be a useful tactic for reducing endothelial adhesion, a characteristic of inflammatory responses. The development of novel therapeutic interventions that reduce leukocyte adhesion and lessen the negative effects of inflammatory diseases may thus result from further elucidation of the underlying mechanistic aspects of the relationship between

endothelial surface molecules and leukocyte infiltration (Munro, 1993). Interleukin-22 (IL-22)-mediated epithelial homeostasis and mucosal wound healing have both been demonstrated to be adversely affected by SOCS3, a crucial negative regulator of many cytokine signaling pathways. To maintain long-term remission in individuals with UC, it may be advantageous to find methods to avoid SOCS3 overexpression. These findings emphasize the critical need for further research into the precise molecular mechanisms governing SOCS3-mediated immunoregulation in the context of inflammatory diseases, with the ultimate objective of creating specialized therapeutic strategies for deregulated SOCS3 expression in UC patients (Xu et al., 2015). In conclusion, the key elements of the ETP for UC treatment are captured by the identified core targets, which show a strong relationship with the pathogenic pathways of UC. These results highlight the critical necessity for ongoing research targeted at enhancing our comprehension of the basic mechanisms causing UC, allowing for the eventual creation of ETP therapies for successfully treating the condition.

Further GO functional analysis indicated that these targets are involved in many biological processes, including response

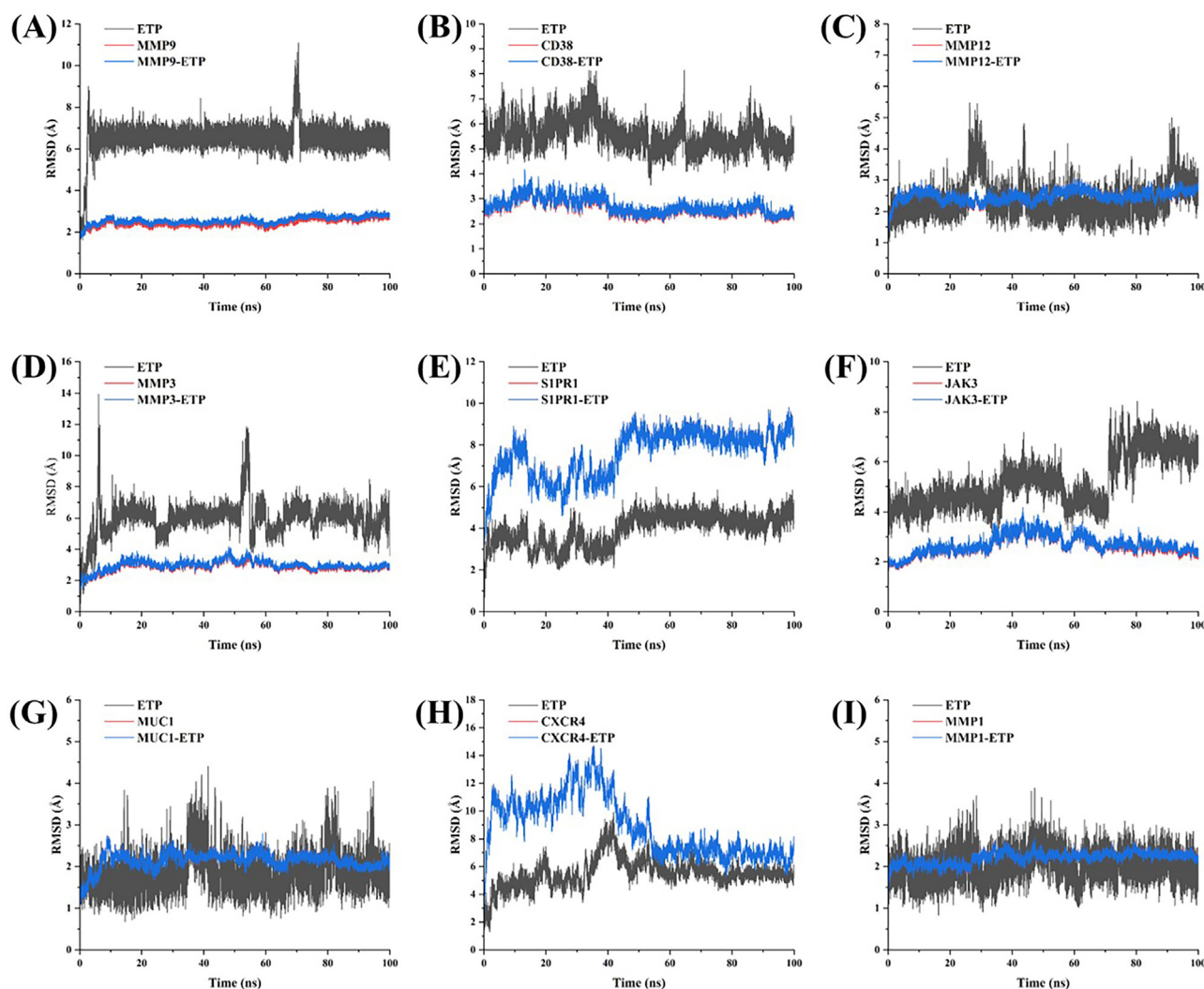


**Fig. 9** RMSD results of ETP binding with target proteins. (A) ETP-MMP9. (B) ETP-CD38. (C) ETP-MMP12. (D) ETP-MMP3. (E) ETP-SIPR1. (F) ETP-JAK3. (G) ETP-MUC1. (H) ETP-CXCR4. (I) ETP-MMP1. The gray color represents the stability of ETP, the red color represents the stability of the protein, and the blue color represents the stability of the receptor-ligand system.

to hypoxia, tissue morphogenesis, cellular response to cytokine stimulus, collagen catabolic process, and positive regulation of cell migration. These biological processes are closely related to the pathological process of UC. In brief, during the pathogenesis of UC, cells are stimulated by cytokines in a series of reactions, along with a significant increase in collagen degradation and specific changes in tissue morphology, which are accompanied by a hypoxic response at the site of inflammation, while impaired epithelial barrier function due to apoptosis and entry of neutrophils lead to further deterioration of UC (Silvennoinen et al., 1996); (Sträter et al., 1997); (van der Steen et al., 2009); (Xue et al., 2013); (Danese and Panés, 2014); (Vitale et al., 2017); (Alvarado et al., 2019). Computing research indicates that the efficient usage of ETP has been found to reduce the symptoms of UC patients by favorably influencing the control of these biological systems.

The results of KEGG analysis showed that ETP can regulate many pathways and exert beneficial effects on UC. It can also inhibit some pathways to suppress the development of uc-related complications, such as cancer and atherosclerosis.

Specifically, the TNF- $\alpha$  signaling pathway, the most extensively studied pathway in IBD, is also the primary target in the development of drugs for related diseases, and TNF- $\alpha$  inhibitors do improve inflammatory symptoms in patients, but mono-anti-TNF therapies are limited (Argollo et al., 2017). IL-17 is closely associated with the upregulation of IFN- $\gamma$ , and the interaction of these inflammatory mediators induces severe colitis in IBD through anti-Drugs that exert efficacy through IL-17 are also in development (Hueber et al., 2012). The recruitment of peripheral leukocytes to the intestine is an important process in intestinal inflammation, and persistent leukocyte tissue infiltration leads to the persistence of a cascade response. It has been demonstrated that intestinal inflammation can be suppressed by blocking leukocyte migration (Oshitani et al., 2002); (Aherne et al., 2012). Ulcerative colitis causes patients to have to take medication for the rest of their lives, and the complications arising from ongoing chronic inflammation are also painful. According to a 30-year follow-up study, patients with IBD have a significantly increased risk of developing gastrointestinal and extraintesti-

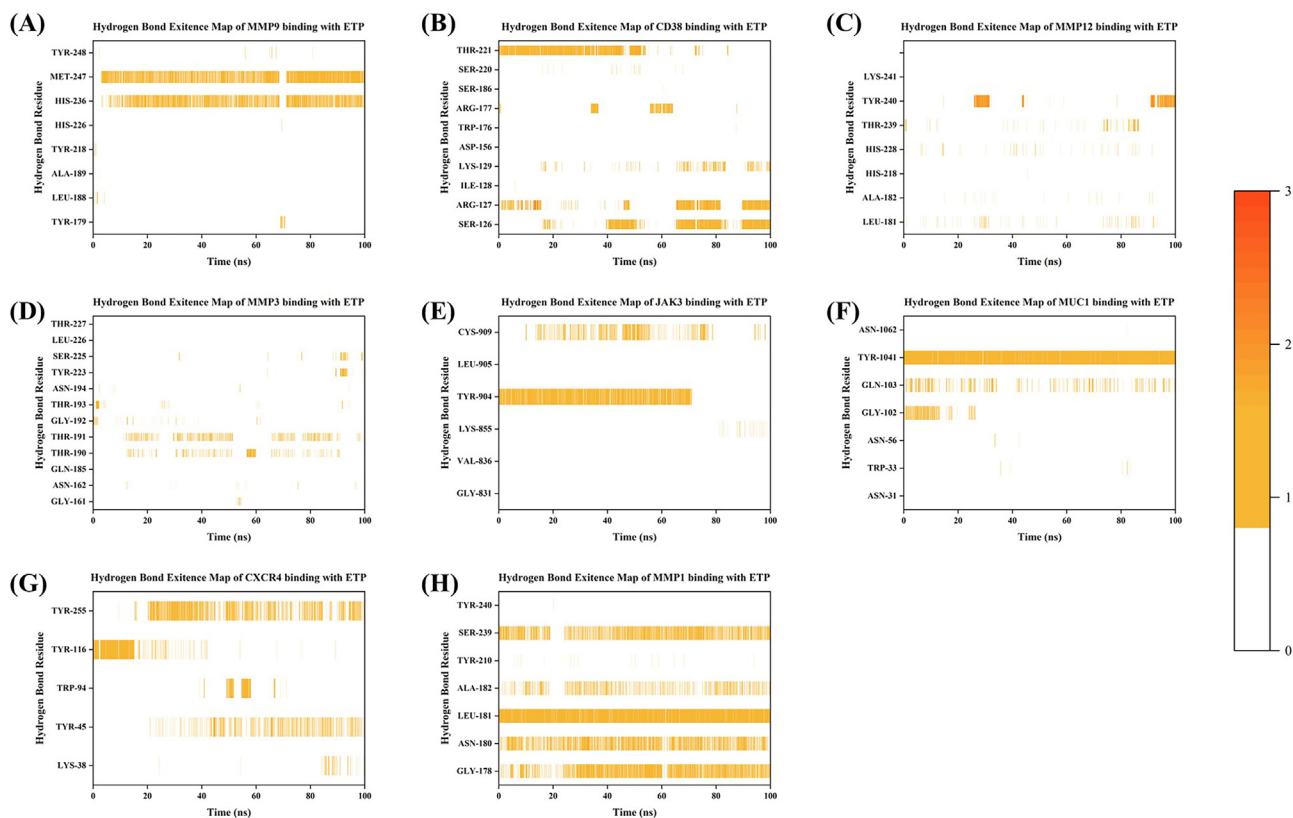


**Fig. 10** Hydrogen bonds of ETP binding with target proteins. (A) ETP-MMP9. (B) ETP-CD38. (C) ETP-MMP12. (D) ETP-MMP3. (E) ETP-JAK3. (F) ETP-MUC1. (G) ETP-CXCR4. (H) ETP-MMP1. The color scale indicates the number of hydrogen bonds.

**Table 3** MM-PBSA results of ETP with key targets.

Target protein	Binding energy (kJ/mol)	Van der Waals energy (kJ/mol)	Electrostatic energy (kJ/mol)	Polar solvation energy (kJ/mol)	SASA energy (kJ/mol)
MMP9	$-84.2963 \pm 11.38565$	$-117.903 \pm 7.852449$	$-38.9861 \pm 8.374826$	$91.46633 \pm 15.79228$	$-18.873 \pm 1.384807$
CD38	$-67.6004 \pm 24.96992$	$-139.077 \pm 14.2074$	$-73.636 \pm 21.20749$	$167.3553 \pm 20.49478$	$-22.2423 \pm 0.966428$
MMP12	$-94.2005 \pm 15.47327$	$-169.304 \pm 12.98226$	$-38.8331 \pm 16.29954$	$137.7041 \pm 16.92731$	$-23.7672 \pm 1.464083$
MMP3	$-45.6328 \pm 24.04062$	$-89.727 \pm 40.5743$	$10.61357 \pm 15.42546$	$46.53195 \pm 22.68081$	$-13.0516 \pm 5.619503$
S1PR1	$-95.9769 \pm 15.04622$	$-188.611 \pm 11.10229$	$-14.6537 \pm 5.88666$	$131.972 \pm 20.35869$	$-24.6843 \pm 0.715044$
JAK3	$-49.0474 \pm 14.50611$	$-124.517 \pm 13.97964$	$-1.25514 \pm 13.98927$	$98.30071 \pm 31.63883$	$-21.576 \pm 1.636458$
MUC1	$-79.676 \pm 21.7837$	$-113.93 \pm 28.17811$	$-36.1207 \pm 12.72225$	$86.28333 \pm 22.7929$	$-15.9084 \pm 3.814098$
CXCR4	$-54.6359 \pm 21.23318$	$-160.497 \pm 13.11832$	$-36.5652 \pm 15.66174$	$165.5769 \pm 25.14471$	$-23.1506 \pm 0.793432$
MMP1	$-87.1345 \pm 15.98618$	$-146.166 \pm 8.102114$	$-53.6983 \pm 11.45997$	$132.7092 \pm 18.41954$	$-19.9799 \pm 0.684544$

nal malignancies (Kappelman et al., 2014). Additionally, patients with IBD have a significantly increased risk of acute mesenteric ischemia, and therefore a greater risk of atherosclerosis (Ha et al., 2009).

Molecular docking was used to assess the binding ability of ETP to 15 key target proteins. The affinity of 12 targets in the docking results was less than  $-6.0$  kcal/mol, indicating that most of the targets may have good binding ability to ETP. Three targets, MMP9, CD38, and MMP12, showed the strongest binding ability. Molecular dynamics simulations were used to further investigate the top nine target proteins (affinity  $< -7.7$  kcal/mol) in molecular docking with affinity to ETP. The combined RMSD, hydrogen bonding, and

MM-PBSA data indicate that ETP exhibits a stable complex structure and strong affinity for five targets, MMP1, MMP9, MUC1, S1PR1, and MMP12. This suggests that ETP may exert anti-inflammatory effects through these targets. We have shown here that ETP has excellent anti-inflammatory properties and that, through a series of computational simulations, it may act on multiple targets and biological processes to prevent the onset of ulcerative colitis. However, additional in vivo tests are still required to confirm these findings. Additionally, we have shown that ETP possesses significant cytotoxicity in addition to its potent anti-inflammatory properties. This might to some extent put a stop to further study and creation of ETP. A strong basis will be created for the use of ETP if its toxicity

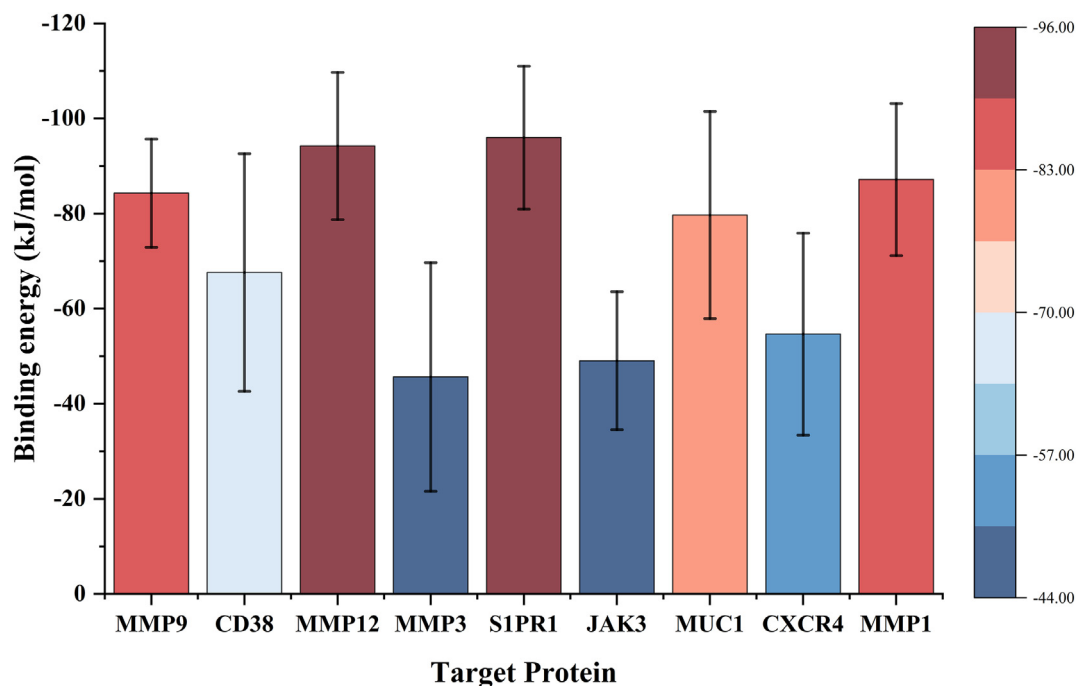


**Fig. 11** Binding energy of ETP with key target proteins. The color scale indicates the strength of binding energy.

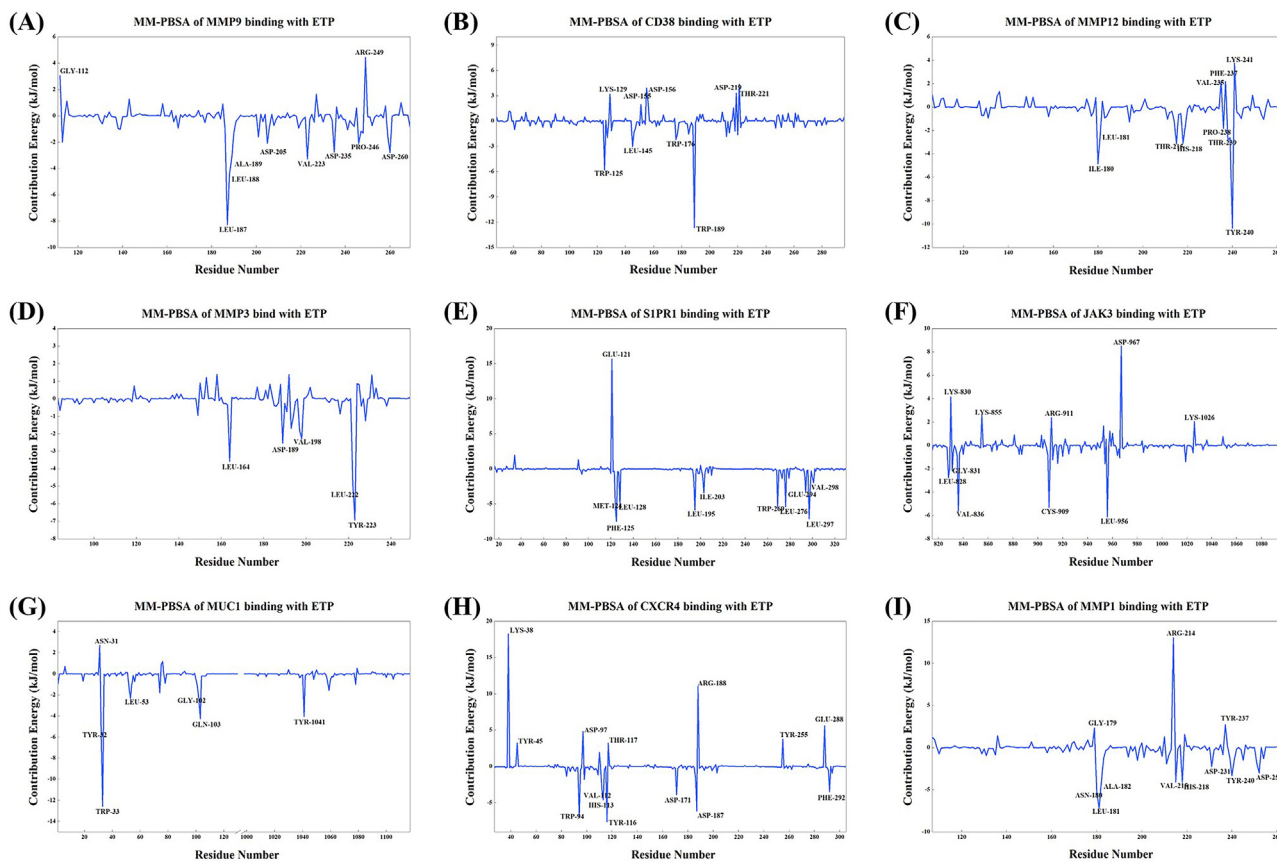


**Fig. 12** Key residues of ETP binding with target proteins in the MM-PBSA results. (A) ETP-MMP9. (B) ETP-CD38. (C) ETP-MMP12. (D) ETP-MMP3. (E) ETP-S1PR1. (F) ETP-JAK3. (G) ETP-MUC1. (H) ETP-CXCR4. (I) ETP-MMP1. The key amino acid residues are all labeled in the figure.

to cells can be decreased by structural alteration without impacting its action.

## 5. Conclusion

The present work reveals the therapeutic potential of ETP, a natural sesquiterpene, by elucidating its effectiveness as a strong anti-inflammatory drug in the context of treating UC.

The main molecular targets and mechanisms of action of ETP were uncovered using network pharmacology, molecular docking, molecular dynamics simulation, and MM-PBSA, and the findings highlight how ETP has several facets and influences a variety of targets in different ways.

The study's findings hold great promise for expanding our knowledge of the therapeutic potential of ETP and opening the door for further investigation into how to best use this bioactive substance to treat UC.

## 6. Authorship contribution statement

Yifei Wang and Cuifang Ye supervised the experiment and designed the study. Jianghao Liu isolated the compounds and investigated the anti-inflammatory activity. Menghe Li completed bioinformatics-related analysis and computation and drafted the manuscript. Caiwenjie La and Tao Liu analyzed the data. Zibo Zhao, Zui Wang, Minghui Dai and Jiming Chen assisted in the experiment. Zhe Ren and Yifei Wang reviewed the final version of the paper. All the authors provided intellectual content and approved the final version of the manuscript.

## Funding

This work was supported by the Guangdong Modern Agricultural Industry Technology System Innovation Team Project of China [2022KJ142] and the Guangzhou Key R&D Program of China [202206010008].

## Declaration of Competing Interest

The authors declare that they have no known competing financial interests or personal relationships that could have appeared to influence the work reported in this paper.

## Acknowledgments

All database and software authors used in this paper are gratefully acknowledged.

## Appendix A. Supplementary material

Supplementary data to this article can be found online at <https://doi.org/10.1016/j.arabjc.2023.105050>.

## References

- Abraham, M.J., Murtola, T., Schulz, R., Páll, S., Smith, J.C., Hess, B., Lindahl, E., 2015. GROMACS: High performance molecular simulations through multi-level parallelism from laptops to supercomputers. *SoftwareX*. 1, 19–25. <https://doi.org/10.1016/j.softx.2015.06.001>.
- Aherne, C.M., Collins, C.B., Masterson, J.C., Tizzano, M., Boyle, T. A., Westrich, J.A., Parnes, J.A., Furuta, G.T., Rivera-Nieves, J., Eltzschig, H.K., 2012. Neuronal guidance molecule netrin-1 attenuates inflammatory cell trafficking during acute experimental colitis. *Gut* 61, 695–705. <https://doi.org/10.1136/gutjnl-2011-300012>.
- Ahmed, A.A., El-Moghazy, S.A., El-Shanawany, M.A., Abdel-Ghani, H.F., Karchesy, J., Sturtz, G., Dalley, K., Paré, P.W., 2004. Polyol monoterpenes and sesquiterpene lactones from the Pacific Northwest plant *Artemisia s uksdorfii*. *J. Nat. Prod.* 67, 1705–1710. <https://doi.org/10.1021/np049954j>.
- Alvarado, D.M., Chen, B., Iticovici, M., Thaker, A.I., Dai, N., VanDussen, K.L., Shaikh, N., Lim, C.K., Guillemin, G.J., Tarr, P. I., Ciorba, M.A., 2019. Epithelial Indoleamine 2,3-Dioxygenase 1 modulates aryl hydrocarbon receptor and notch signaling to increase differentiation of secretory cells and alter mucus-associated microbiota. *Gastroenterology* 157. <https://doi.org/10.1053/j.gastro.2019.07.013>.
- Amberger, J.S., Bocchini, C.A., Schiettecatte, F., Scott, A.F., Hamosh, A., 2015. OMIM.org: Online Mendelian Inheritance in Man (OMIM®), an online catalog of human genes and genetic disorders. *Nucleic Acids Res.* 43, D789–D798. <https://doi.org/10.1093/nar/gku1205>.
- Argollo, M., Fiorino, G., Hindryckx, P., Peyrin-Biroulet, L., Danese, S., 2017. Novel therapeutic targets for inflammatory bowel disease. *J. Autoimmun.* 85, 103–116. <https://doi.org/10.1016/j.jaut.2017.07.004>.
- Barrett, T., Wilhite, S.E., Ledoux, P., Evangelista, C., Kim, I.F., Tomashevsky, M., Marshall, K.A., Phillippy, K.H., Sherman, P. M., Holko, M., Yefanov, A., Lee, H., Zhang, N., Robertson, C.L., Serova, N., Davis, S., Soboleva, A., 2013. NCBI GEO: archive for functional genomics data sets—update. *Nucleic Acids Res.* 41, D991–D995. <https://doi.org/10.1093/nar/gks1193>.
- Benkiki, N., Kabouche, Z., Bruneau, C., 2007. Two coumarins and a thienylbutylamide from *Anacyclus cyrtolopioides* from the Algerian Septentrional Sahara. *Chem. Natural Compounds* 43, 612–613. <https://doi.org/10.1007/s10600-007-0205-z>.
- Biancheri, P., Brezski, R.J., Di Sabatino, A., Greenplate, A.R., Soring, K.L., Corazza, G.R., Kok, K.B., Rovedatti, L., Vossenkämper, A., Ahmad, N., Snoek, S.A., Vermeire, S., Rutgeerts, P., Jordan, R.E., MacDonald, T.T., 2015. Proteolytic cleavage and loss of function of biologic agents that neutralize tumor necrosis factor in the mucosa of patients with inflammatory bowel disease. *Gastroenterology* 149. <https://doi.org/10.1053/j.gastro.2015.07.002>.
- Breugelmans, T., Van Spaendonk, H., De Man, J.G., De Schepper, H. U., Jauregui-Amezaga, A., Macken, E., Lindén, S.K., Pintelon, I., Timmermans, J.-P., De Winter, B.Y., Smet, A., 2020. In-Depth study of transmembrane mucins in association with intestinal barrier dysfunction during the course of T Cell transfer and DSS-Induced Colitis. *J. Crohns Colitis* 14, 974–994. <https://doi.org/10.1093/ecco-jcc/jjaa015>.
- Brown, G., 1992. Two new compounds from *Artemisia annua*. *J. Nat. Prod.* 55, 1756–1760. <https://doi.org/10.1021/np50090a006>.
- Case, D., Aktulga, H., Belfon, K., Ben-Shalom, I., Brozell, S., Cerutti, D., Cheatham III, T., Cisneros, G., Cruzeiro, V., Darden, T., 2022. AmberTools22. University of California, San Francisco.
- Castaneda, F.E., Walia, B., Vijay-Kumar, M., Patel, N.R., Roser, S., Kolachala, V.L., Rojas, M., Wang, L., Oprea, G., Garg, P., Gewirtz, A.T., Roman, J., Merlin, D., Sitaraman, S.V., 2005. Targeted deletion of metalloproteinase 9 attenuates experimental colitis in mice: central role of epithelial-derived MMP. *Gastroenterology* 129, 1991–2008.
- Chen, P., Bai, Q., Wu, Y., Zeng, Q., Song, X., Guo, Y., Zhou, P., Wang, Y., Liao, X., Wang, Q., Ren, Z., Wang, Y., 2021. The Essential Oil of *Artemisia argyi* H.Lév. and Vaniot Attenuates

- NLRP3 Inflammasome Activation in THP-1 Cells. *Front. Pharmacol.* 12,. <https://doi.org/10.3389/fphar.2021.712907>
- Craveir, A., Vieira, I., 1992. Synthesis of (-)-Juvabione and (-)-Epi-Juvabione. *J. Braz. Chem. Soc.*, 124–126 <https://doi.org/10.5935/0103-5053.19920027>.
- Danese, S., Panés, J., 2014. Development of drugs to target interactions between leukocytes and endothelial cells and treatment algorithms for inflammatory bowel diseases. *Gastroenterology* 147, 981–989. <https://doi.org/10.1053/j.gastro.2014.08.044>.
- Eberhardt, J., Santos-Martins, D., Tillack, A.F., Forli, S., 2021. AutoDock Vina 1.2.0: New Docking Methods, Expanded Force Field, and Python Bindings. *J. Chem. Inf. Model.* 61, 3891–3898. <https://doi.org/10.1021/acs.jcim.1c00203>.
- Eldehna, W.M., El Hassab, M.A., Abo-Ashour, M.F., Al-Warhi, T., Elaasser, M.M., Safwat, N.A., Suliman, H., Ahmed, M.F., Al-Rashood, S.T., Abdel-Aziz, H.A., El-Haggag, R., 2021. Development of isatin-thiazolo[3,2-a]benzimidazole hybrids as novel CDK2 inhibitors with potent in vitro apoptotic anti-proliferative activity: synthesis, biological and molecular dynamics investigations. *Bioorg. Chem.* 110,. <https://doi.org/10.1016/j.bioorg.2021.104748>
- Fan, T.-T., Cheng, B.-L., Fang, X.-M., Chen, Y.-C., Su, F., 2020. Application of Chinese medicine in the management of critical conditions: a review on sepsis. *Am. J. Chin. Med.* 48, 1315–1330. <https://doi.org/10.1142/S0192415X20500640>.
- Formisano, C., Rigano, D., Senatore, F., Bancheva, S., Maggio, A., Rosselli, S., Bruno, M., 2012. Flavonoids in Subtribe Centaureinae (Cass.) Dumort. (Tribe Cardueae, Asteraceae): Distribution and 13C-NMR Spectral Data. *Chem. Biodivers.* 9, 2096. <https://doi.org/10.1002/cbdv.201100208>.
- Gerner, R.R., Klepsch, V., Macheiner, S., Arnhard, K., Adolph, T.E., Grander, C., Wieser, V., Pfister, A., Moser, P., Hermann-Kleiter, N., Baier, G., Oberacher, H., Tilg, H., Moschen, A.R., 2018. NAD metabolism fuels human and mouse intestinal inflammation. *Gut* 67, 1813–1823. <https://doi.org/10.1136/gutjnl-2017-314241>.
- Gfeller, D., Michielin, O., Zoete, V., 2013. Shaping the interaction landscape of bioactive molecules. *Bioinformatics* 29, 3073–3079. <https://doi.org/10.1093/bioinformatics/btt540>.
- Ha, C., Magowan, S., Accortt, N.A., Chen, J., Stone, C.D., 2009. Risk of arterial thrombotic events in inflammatory bowel disease. *Am. J. Gastroenterol.* 104, 1445–1451. <https://doi.org/10.1038/ajg.2009.81>.
- Habtemariam, S., 2001. Antiinflammatory activity of the antirheumatic herbal drug, gravel root (*Eupatorium purpureum*): further biological activities and constituents. *Phytother. Res.* 15, 687–690. <https://doi.org/10.1002/ptr.887>.
- Higashinakasu, K., Yamada, K., Shigemori, H., Hasegawa, K., 2005. Isolation and identification of potent stimulatory allelopathic substances exuded from germinating burdock (*Arctium lappa*) seeds. *Heterocycles* 65, 1431–1438.
- Hiraga, Y., Chen, L., Kurokawa, M., Ohta, S., Suga, T., Hirata, T., 1996. Structure-activity relationships of cinnamic acid derivatives as germination inhibitor of the fern *Gleichenia japonica*. *Nat. Prod. Lett.* 9, 21–26. <https://doi.org/10.1080/10575639608043573>.
- Hueber, W., Sands, B.E., Lewitzky, S., Vandemeulebroecke, M., Reinisch, W., Higgins, P.D.R., Wehkamp, J., Feagan, B.G., Yao, M.D., Karczewski, M., Karczewski, J., Pezous, N., Bek, S., Bruin, G., Mellgard, B., Berger, C., Londei, M., Bertolino, A.P., Tougas, G., Travis, S.P.L., 2012. Secukinumab, a human anti-IL-17A monoclonal antibody, for moderate to severe Crohn's disease: unexpected results of a randomised, double-blind placebo-controlled trial. *Gut* 61, 1693–1700. <https://doi.org/10.1136/gutjnl-2011-301668>.
- Iverson, C.D., Zahid, S., Li, Y., Shoqafi, A.H., Ata, A., Samarasekera, R., 2010. Glutathione S-transferase inhibitory, free radical scavenging, and anti-leishmanial activities of chemical constituents of *Artocarpus nobilis* and *Matricaria chamomilla*. *Phytochem. Lett.* 3, 207–211. <https://doi.org/10.1016/j.phytol.2010.07.008>.
- Jiang, S., Wang, M.-Y., Zafar, S., Xie, Q.-L., Jian, Y.-Q., Yuan, H.-W., Li, B., Peng, C.-Y., Chen, W.-M., Liu, B., 2022. Structural elucidation, antioxidant and hepatoprotective activities of chemical composition from Jinsi Huangju (*Chrysanthemum morifolium*) flowers. *Arab. J. Chem.* 15,. <https://doi.org/10.1016/j.arabjc.2022.104292>
- Jin, H.Z., Lee, J.H., Lee, D., et al, 2004. Inhibitors of the LPS-induced NF-kappaB activation from *Artemisia sylvatica*. *Phytochemistry* 65, 2247–2253. <https://doi.org/10.1016/j.phytochem.2004.06.034>.
- Kang, U., Park, J., Han, A.-R., Woo, M.H., Lee, J.-H., Lee, S.K., Chang, T.-S., Woo, H.A., Seo, E.K., 2016. Identification of cytoprotective constituents of the flower buds of *Tussilago farfara* against glucose oxidase-induced oxidative stress in mouse fibroblast NIH3T3 cells and human keratinocyte HaCaT cells. *Arch. Pharm. Res.* 39, 474–480. <https://doi.org/10.1007/s12272-016-0730-z>.
- Kappelman, M.D., Farkas, D.K., Long, M.D., Erichsen, R., Sandler, R.S., Sørensen, H.T., Baron, J.A., 2014. Risk of cancer in patients with inflammatory bowel diseases: a nationwide population-based cohort study with 30 years of follow-up evaluation. *Clin. Gastroenterol. Hepatol.* 12. <https://doi.org/10.1016/j.cgh.2013.03.034>.
- Ke, Z., Xiao-Qing, C., Peng-Fei, T., 2012. A new 1, 10-secoguaianolide from the aerial parts of *Artemisia anomala*. *Chin. J. Nat. Med.* 10, 358–362. [https://doi.org/10.1016/S1875-5364\(12\)60071-5](https://doi.org/10.1016/S1875-5364(12)60071-5).
- Keir, M.E., Fuh, F., Ichikawa, R., Acres, M., Hackney, J.A., Hulme, G., Carey, C.D., Palmer, J., Jones, C.J., Long, A.K., Jiang, J., Klabunde, S., Mansfield, J.C., Looney, C.M., Faubion, W.A., Filby, A., Kirby, J.A., McBride, J., Lamb, C.A., 2021. Regulation and Role of  $\alpha$ E Integrin and Gut Homing Integrins in Migration and Retention of Intestinal Lymphocytes during Inflammatory Bowel Disease. *J. Immunol.* 207, 2245–2254. <https://doi.org/10.4049/jimmunol.2100220>.
- Kiyota, H., Yoneta, Y., Oritani, T., 1997. Synthesis and biological activities of methyl 3, 7-and 4, 5-didehydrojasmonates. *Phytochemistry* 46, 983–986. [https://doi.org/10.1016/S0031-9422\(97\)00374-9](https://doi.org/10.1016/S0031-9422(97)00374-9).
- Kriegelstein, C.F., Cerwinka, W.H., Laroux, F.S., Salter, J.W., Russell, J.M., Schuermann, G., Grisham, M.B., Ross, C.R., Granger, D.N., 2001. Regulation of murine intestinal inflammation by reactive metabolites of oxygen and nitrogen: divergent roles of superoxide and nitric oxide. *J. Exp. Med.* 194, 1207–1218.
- Langhorst, J., Wulfert, H., Lauche, R., Klose, P., Cramer, H., Dobos, G.J., Korzenik, J., 2015. Systematic review of complementary and alternative medicine treatments in inflammatory bowel diseases. *J. Crohns Colitis* 9. <https://doi.org/10.1093/ecco-jcc/jju007>.
- Li, Y., Wang, F., Zhang, P.Z., Yang, M., 2015. Chemical constituents from *Periplaneta americana*. *Zhongyaocai.* 38, 2038–2041. <https://doi.org/10.13863/j.issn1001-4454.2015.10.006>.
- Li, Y.-P., Zhang, Y.-M., Liu, Y., Chen, Y.-G., 2007. Chemical constituents of *Dendrobium crystallium*. *Chem. Nat. Compd.* 43, 698–699. <https://doi.org/10.1007/s10600-007-0234-7>.
- Liang, J., Nagahashi, M., Kim, E.Y., Harikumar, K.B., Yamada, A., Huang, W.-C., Hait, N.C., Allegood, J.C., Price, M.M., Avni, D., Takabe, K., Kordula, T., Milstien, S., Spiegel, S., 2013. Sphingosine-1-phosphate links persistent STAT3 activation, chronic intestinal inflammation, and development of colitis-associated cancer. *Cancer Cell* 23, 107–120. <https://doi.org/10.1016/j.ccr.2012.11.013>.
- Lichtenstein, G.R., Rutgeerts, P., Sandborn, W.J., Sands, B.E., Diamond, R.H., Blank, M., Montello, J., Tang, L., Cornillie, F., Colombel, J.-F., 2012. A pooled analysis of infections, malignancy, and mortality in infliximab- and immunomodulator-treated adult patients with inflammatory bowel disease. *Am. J. Gastroenterol.* 107, 1051–1063. <https://doi.org/10.1038/ajg.2012.89>.
- Liu, Y., He, Y., Wang, F., Xu, R., Yang, M., Ci, Z., Wu, Z., Zhang, D., Lin, J., 2021. From longevity grass to contemporary soft gold: Explore the chemical constituents, pharmacology, and toxicology of *Artemisia argyi* H.Lév. & vaniot essential oil. *J. Ethnopharmacol.* 279,. <https://doi.org/10.1016/j.jep.2021.114404>

- Marques, M.R., Stüker, C., Kichik, N., Tarragó, T., Giralt, E., Morel, A.F., Dalcol, I.I., 2010. Flavonoids with prolyl oligopeptidase inhibitory activity isolated from *Scutellaria racemosa* Pers. *Fitoterapia* 81, 552–556. <https://doi.org/10.1016/j.fitote.2010.01.018>.
- Marshall, D.C., Lyman, S.K., McCauley, S., Kovalenko, M., Spangler, R., Liu, C., Lee, M., O'Sullivan, C., Barry-Hamilton, V., Ghermazien, H., Mikels-Vigdal, A., Garcia, C.A., Jorgensen, B., Velayo, A.C., Wang, R., Adamkewicz, J.I., Smith, V., 2015. Selective allosteric inhibition of MMP9 is efficacious in preclinical models of ulcerative colitis and colorectal cancer. *PLoS One* 10, e0127063.
- Mikami, S., Nakase, H., Yamamoto, S., Takeda, Y., Yoshino, T., Kasahara, K., Ueno, S., Uza, N., Oishi, S., Fujii, N., Nagasawa, T., Chiba, T., 2008. Blockade of CXCL12/CXCR4 axis ameliorates murine experimental colitis. *J. Pharmacol. Exp. Ther.* 327, 383–392. <https://doi.org/10.1124/jpet.108.141085>.
- Munro, J.M., 1993. Endothelial-leukocyte adhesive interactions in inflammatory diseases. *Eur. Heart J.* 14 (Suppl K), 72–77.
- Ng, S.C., Lam, Y.T., Tsoi, K.K.F., Chan, F.K.L., Sung, J.J.Y., Wu, J. C.Y., 2013. Systematic review: the efficacy of herbal therapy in inflammatory bowel disease. *Aliment. Pharmacol. Ther.* 38, 854–863. <https://doi.org/10.1111/apt.12464>.
- Oshitani, N., Hato, F., Kitagawa, S., Masuyama, J., Higuchi, K., Matsumoto, T., Arakawa, T., 2002. Expression of 4C8 antigen, a novel transendothelial migration-associated molecule on activated T lymphocytes, in inflammatory bowel disease. *J. Pathol.* 197, 589–594.
- Pérez-Jeldres, T., Tyler, C.J., Boyer, J.D., Karuppuchamy, T., Yarur, A., Giles, D.A., Yeasmin, S., Lundborg, L., Sandborn, W.J., Patel, D.R., Rivera-Nieves, J., 2019. Targeting Cytokine Signaling and Lymphocyte Traffic via Small Molecules in Inflammatory Bowel Disease: JAK Inhibitors and S1PR Agonists. *Front. Pharmacol.* 10, 212. <https://doi.org/10.3389/fphar.2019.00212>.
- Piñero, J., Saüch, J., Sanz, F., Furlong, L.I., 2021. The DisGeNET cytoscape app: exploring and visualizing disease genomics data. *Comput. Struct. Biotechnol. J.* 19, 2960–2967. <https://doi.org/10.1016/j.csbj.2021.05.015>.
2019. Protein Data Bank: the single global archive for 3D macromolecular structure data. *Nucleic Acids Res.* 47, D520–D528. <https://doi.org/10.1093/nar/gky949>.
- Roskoski, R., 2016. Janus kinase (JAK) inhibitors in the treatment of inflammatory and neoplastic diseases. *Pharmacol. Res.* 111, 784–803. <https://doi.org/10.1016/j.phrs.2016.07.038>.
- Seeliger, D., de Groot, B.L., 2010. Ligand docking and binding site analysis with PyMOL and Autodock/Vina. *J. Comput. Aided Mol. Des.* 24, 417–422. <https://doi.org/10.1007/s10822-010-9352-6>.
- Shannon, P., Markiel, A., Ozier, O., Baliga, N.S., Wang, J.T., Ramage, D., Amin, N., Schwikowski, B., Ideker, T., 2003. Cytoscape: a software environment for integrated models of biomolecular interaction networks. *Genome Res.* 13, 2498–2504. <https://doi.org/10.1101/gr.1239303>.
- Shi, W., Han, G.-Q., 1996. Chemical constituents of *Tussilago farfara* L. *J. Chin. Pharm. Sci.* 5, 63–67.
- Shuhua, Q., Dagang, W., Xiaodong, L.J.N.P.R., 2004. Coumarins and ellagic acids from *Sapium chihisianianum* S Lee. *Natural Product Res. Dev.* 16, 297–299.
- Silva, L.A.L., Faqueti, L.G., Reginatto, F.H., Santos, A.D.C.D., Barison, A., Biavatti, M.W., 2015. Phytochemical analysis of *Vernonanthura tweediana* and a validated UPLC-PDA method for the quantification of eriodictyol. *Rev. Bras* 25, 375–381. <https://doi.org/10.1016/j.bjp.2015.07.009>.
- Silvennoinen, J., Risteli, L., Karttunen, T., Risteli, J., 1996. Increased degradation of type I collagen in patients with inflammatory bowel disease. *Gut* 38, 223–228. <https://doi.org/10.1136/gut.38.2.223>.
- Sousa da Silva, A.W., Vranken, W.F., 2012. ACPYPE - AnteChamber PYthon Parser interface. *BMC. Res. Notes* 5, 367. <https://doi.org/10.1186/1756-0500-5-367>.
- Sousa, C., Leitão, A.J., Neves, B.M., Judas, F., Cavaleiro, C., Mendes, A.F., 2020. Standardised comparison of limonene-derived monoterpenes identifies structural determinants of anti-inflammatory activity. *Sci. Rep.* 10, 1–14. <https://doi.org/10.1038/s41598-020-64032-1>.
- Stelzer, G., Rosen, N., Plaschkes, I., Zimmerman, S., Twik, M., Fishilevich, S., Stein, T.I., Nudel, R., Lieder, I., Mazor, Y., Kaplan, S., Dahary, D., Warshawsky, D., Guan-Golan, Y., Kohn, A., Rappaport, N., Safran, M., Lancet, D., 2016. The GeneCards suite: from gene data mining to disease genome sequence analyses. *Curr. Protoc. Bioinformatics* 54. <https://doi.org/10.1002/cpbi.5>.
- Sträter, J., Wellisch, I., Riedl, S., Walczak, H., Koretz, K., Tandara, A., Krammer, P.H., Möller, P., 1997. CD95 (APO-1/Fas)-mediated apoptosis in colon epithelial cells: a possible role in ulcerative colitis. *Gastroenterology* 113, 160–167. [https://doi.org/10.1016/S0016-5085\(97\)70091-X](https://doi.org/10.1016/S0016-5085(97)70091-X).
- Szklarczyk, D., Gable, A.L., Nastou, K.C., Lyon, D., Kirsch, R., Pyysalo, S., Doncheva, N.T., Legeay, M., Fang, T., Bork, P., Jensen, L.J., von Mering, C., 2021. The STRING database in 2021: customizable protein-protein networks, and functional characterization of user-uploaded gene/measurement sets. *Nucleic Acids Res.* 49, D605–D612. <https://doi.org/10.1093/nar/gkaa1074>.
- Toruner, M., Loftus, E.V., Harmsen, W.S., Zinsmeister, A.R., Orenstein, R., Sandborn, W.J., Colombel, J.-F., Egan, L.J., 2008. Risk factors for opportunistic infections in patients with inflammatory bowel disease. *Gastroenterology* 134, 929–936. <https://doi.org/10.1053/j.gastro.2008.01.012>.
- Trott, O., Olson, A.J., 2010. AutoDock Vina: improving the speed and accuracy of docking with a new scoring function, efficient optimization, and multithreading. *J. Comput. Chem.* 31, 455–461. <https://doi.org/10.1002/jcc.21334>.
- Valdés-Tresanco, M.S., Valdés-Tresanco, M.E., Valiente, P.A., Moreno, E., 2021. gmx\_MMPBSA: a new tool to perform end-state free energy calculations with GROMACS. *J. Chem. Theory Comput.* 17, 6281–6291. <https://doi.org/10.1021/acs.jctc.1c00645>.
- van der Steen, L., Tuk, C.W., Bakema, J.E., Kooij, G., Reijkerk, A., Vidarsson, G., Bouma, G., Kraal, G., de Vries, H.E., Beelen, R.H. J., van Egmond, M., 2009. Immunoglobulin A: Fc(alpha)RI interactions induce neutrophil migration through release of leukotriene B4. *Gastroenterology* 137. <https://doi.org/10.1053/j.gastro.2009.06.047>.
- Vitale, S., Strisciuglio, C., Pisapia, L., Miele, E., Barba, P., Vitale, A., Cenni, S., Bassi, V., Maglio, M., Del Pozzo, G., Troncone, R., Staiano, A., Gianfrani, C., 2017. Cytokine production profile in intestinal mucosa of paediatric inflammatory bowel disease. *PLoS One* 12, e0182313.
- von Lampe, B., Barthel, B., Coupland, S.E., Riecken, E.O., Rosewicz, S., 2000. Differential expression of matrix metalloproteinases and their tissue inhibitors in colon mucosa of patients with inflammatory bowel disease. *Gut* 47, 63–73.
- Wan, Y., Liu, Z., Wu, A., Khan, A.H., Zhu, Y., Ding, S., Li, X., Zhao, Y., Dai, X., Zhou, J., Liu, J., Li, Y., Gong, X., Liu, M., Tian, X.-L., 2022. Hyperglycemia promotes endothelial cell senescence through AQR/PLAU signaling axis. *Int. J. Mol. Sci.* 23. <https://doi.org/10.3390/ijms23052879>.
- Wang, X., Shen, Y., Wang, S., Li, S., Zhang, W., Liu, X., Lai, L., Pei, J., Li, H., 2017. PharmMapper 2017 update: a web server for potential drug target identification with a comprehensive target pharmacophore database. *Nucleic Acids Res.* 45, W356–W360. <https://doi.org/10.1093/nar/gkx374>.
- Wang, Y.-D., Yan, P.-Y., 2006. Expression of matrix metalloproteinase-1 and tissue inhibitor of metalloproteinase-1 in ulcerative colitis. *World J. Gastroenterol.* 12, 6050–6053.
- Wang, Y., Yuan, Y., Wang, W., He, Y., Zhong, H., Zhou, X., Chen, Y., Cai, X.-J., Liu, L.-Q., 2022. Mechanisms underlying the therapeutic effects of Qingfei Yin in treating acute lung injury based on GEO datasets, network pharmacology and molecular docking.

- Comput. Biol. Med. 145,. <https://doi.org/10.1016/j.compbiomed.2022.105454> 105454.
- Wu, Y.-T., Zhong, L.-S., Huang, C., Guo, Y.-Y., Jin, F.-J., Hu, Y.-Z., Zhao, Z.-B., Ren, Z., Wang, Y.-F., 2022.  $\beta$ -Caryophyllene Acts as a Ferroptosis Inhibitor to Ameliorate Experimental Colitis. *Int. J. Mol. Sci.* 23. <https://doi.org/10.3390/ijms232416055>.
- Xiao, Y., Lian, H., Zhong, X.S., Krishnachaitanya, S.S., Cong, Y., Dashwood, R.H., Savidge, T.C., Powell, D.W., Liu, X., Li, Q., 2022. Matrix metalloproteinase 7 contributes to intestinal barrier dysfunction by degrading tight junction protein Claudin-7. *Front. Immunol.* 13, 1020902. <https://doi.org/10.3389/fimmu.2022.1020902>.
- Xu, W., Jin, H., Zhang, W., Fu, J., Hu, X., Zhang, W., Yan, S., Shen, Y., 2008. Studies on the chemical constituents of *Daphne pedunculata*. *Chem. Nat. Compd.* 44, 771–772. <https://doi.org/10.1007/s10600-009-9176-6>.
- Xu, A.T., Li, Y., Zhao, D., Shen, J., Xu, X.T., Qiao, Y.Q., Zhu, M.M., Wang, T.R., Cui, Y., Ai, L.Y., Ran, Z.H., 2015. High suppressor of cytokine signaling-3 expression impairs STAT3-dependent protective effects of interleukin-22 in ulcerative colitis in remission. *Inflamm. Bowel Dis.* 21, 241–250. <https://doi.org/10.1097/MIB.0000000000000267>.
- Xue, X., Ramakrishnan, S., Anderson, E., Taylor, M., Zimmermann, E.M., Spence, J.R., Huang, S., Greenson, J.K., Shah, Y.M., 2013. Endothelial PAS domain protein 1 activates the inflammatory response in the intestinal epithelium to promote colitis in mice. *Gastroenterology* 145, 831–841. <https://doi.org/10.1053/j.gastro.2013.07.010>.
- Yao, Z.-J., Dong, J., Che, Y.-J., Zhu, M.-F., Wen, M., Wang, N.-N., Wang, S., Lu, A.-P., Cao, D.-S., 2016. TargetNet: a web service for predicting potential drug-target interaction profiling via multi-target SAR models. *J. Comput. Aided Mol. Des.* 30, 413–424. <https://doi.org/10.1007/s10822-016-9915-2>.
- Yrjänheikki, E., 1980. The reaction of certain pinenes with dimethylamine and formaldehyde. *Acta Universitatis Ouluensis. A, Scientiae rerum naturalium*, 88.
- Zdero, C., Bohlmann, F., 1990. Glaucolides, fulvenogaianolides and other sesquiterpene lactones from *Pentzia* species. *Phytochemistry* 29, 189–194. [https://doi.org/10.1016/0031-9422\(90\)89035-8](https://doi.org/10.1016/0031-9422(90)89035-8).
- Zhang, J., Liang, Y., Liao, X.-J., Deng, Z., Xu, S.-H., 2014. Isolation of a new butenolide from the South China Sea gorgonian coral *Subergorgia suberosa*. *Nat. Prod. Res.* 28, 150–155. <https://doi.org/10.1080/14786419.2013.857668>.
- Zhao, M., Zhang, X., Wang, Y., Huang, M., Duan, J.-A., Gödecke, T., Szymulanska-Ramamurthy, K.M., Yin, Z., Che, C.-T., 2014. Germacranes and m-menthane from *Illicium lanceolatum*. *Molecules* 19, 4326–4337. <https://doi.org/10.3390/molecules19044326>.
- Zhou, Y., Zhou, B., Pache, L., Chang, M., Khodabakhshi, A.H., Tanaseichuk, O., Benner, C., Chanda, S.K., 2019. Metascape provides a biologist-oriented resource for the analysis of systems-level datasets. *Nat. Commun.* 10, 1523. <https://doi.org/10.1038/s41467-019-09234-6>.
- Zhu, D., Xia, Y., Li, S., et al, 2022. Iso-seco-tanaparholide activates Nrf2 signaling pathway through Keap1 modification and oligomerization to exert anti-inflammatory effects. *Free Radic. Biol. Med.* 178, 398–412. <https://doi.org/10.1016/j.freeradbiomed.2021.12.259>.